STOCHASTIC RESONANCE IN CHUA'S CIRCUIT DRIVEN BY ALPHA-STABLE NOISE

A Thesis Submitted to
the Graduate School of Engineering and Sciences of
İzmir Institute of Technology
in Partial Fulfillment of the Requirements for the Degree of

MASTER OF SCIENCE

in Electronics and Communication Engineering

by
Serpil YILMAZ

July 2012
İZMİR

We approve the thesis of **Serpil YILMAZ**

Examining Committee Members:

Prof. Dr. Ferit Acar SAVACI
Department of Electrical and Electronics Engineering,
İzmir Institute of Technology

Assist. Prof. Dr. Mustafa A. ALTINKAYA
Department of Electrical and Electronics Engineering,
İzmir Institute of Technology

Assist. Prof. Dr. M. Emre ÇEK
Department of Electrical and Electronics Engineering,
Dokuz Eylül University

10 July 2012

Prof. Dr. Ferit Acar SAVACI
Supervisor, Department of Electrical and Electronics Engineering,
İzmir Institute of Technology

Prof. Dr. Ferit Acar SAVACI
Head of the Department of
Electrical and Electronics Engineering

Prof. Dr. R. Tuğrul SENGER
Dean of the Graduate School of
Engineering and Sciences

ACKNOWLEDGEMENTS

I would like to express my sincere gratitude to my advisor Prof. Dr. Ferit Acar SAVACI for the continuous support of my research and thesis, for his patience, motivation, enthusiasm, and immense knowledge. It has been an honor for me to have an opportunity to work with such a great advisor. I appreciate all his contributions of time and idea to make my thesis experience productive and enlightening.

I would like to thank my committee members Assist.Prof.Dr. Mustafa A. ALTINKAYA and Assist.Prof.Dr. Emre ÇEK for their contributions.

I would also like to thank TÜBİTAK-BİDEB for awarding me with their graduate scholarship.

I am very grateful to Olcay Duman for his never-ending support and encouragement.

Last but not least, I would like to thank my parents and my sister Zeynep Yılmaz for their endless love and support.

ABSTRACT

STOCHASTIC RESONANCE IN CHUA'S CIRCUIT
DRIVEN BY ALPHA-STABLE NOISE

The main aim of this thesis is to investigate the stochastic resonance (SR) in Chua's circuit driven by alpha-stable noise which has better approximation to a real-world signal than Gaussian distribution. SR is a phenomenon in which the response of a nonlinear system to a sub-threshold (weak) input signal is enhanced with the addition of an optimal amount of noise. There have been an increasing amount of applications based on SR in various fields. Almost all studies related to SR in chaotic systems assume that the noise is Gaussian, which leads researchers to investigate the cases in which the noise is non-Gaussian hence has infinite variance. In this thesis, the spectral power amplification which is used to quantify the SR has been evaluated through fractional lower order Wigner Ville distribution of the response of a system and analyzed for various parameters of alpha-stable noise. The results provide a visible SR effect in Chua's circuit driven by symmetric and skewed-symmetric alpha-stable noise distributions. Furthermore, a series of simulations reveal that the mean residence time that is the average time spent by the trajectory in an attractor can vary depending on different alpha-stable noise parameters.

ÖZET

ALPHA-KARARLI GÜRÜLTÜYLE SÜRÜLMÜŞ CHUA DEVRESİNDE STOKASTİK REZONANS

Bu tezdeki temel amaç gerçek hayattaki sinyallere Gauss dağılımından daha iyi yaklaşım veren alpha-kararlı gürültüyle sürülmüş Chua devresinde stokastik rezonansı (SR) incelemektir. SR olgusu doğrusal olmayan dinamik sistemlerin zayıf sinyallere karşı performansının ek gürültüyle arttırılmasıdır. SR'a dayalı uygulamalar çeşitli alanlarda gittikçe artmaktadır. SR ile ilgili kaotik sistemlerde yapılan çalışmaların çoğu gürültünün Gauss olduğunu varsaymaktadır. Bu durum gürültünün Gauss olmadığı dolayısıyla sonsuz varyansa sahip olduğu durumları incelemeye yönlendirmiştir. Bu tezde, SR etkisini gözlemlemek için kullanılan spektral güç yükseltimi için sistem tepkisinin kesirli düşük mertebeli Wigner Ville dağılımı hesaplanmış ve çeşitli alpha-kararlı gürültü parametrelerine bağlı olarak analiz edilmiştir. Sonuçlar alpha-kararlı simetrik ve simetrik olmayan gürültüyle sürülmüş Chua devresinde gözle görülür bir SR etkisi sağladığını göstermiştir. Ayrıca tek bir çekicide ortalama kalma süresinin çeşitli alpha-kararlı gürültü parametrelerine bağlı olarak değişebileceği gözlemlenmiştir.

TABLE OF CONTENTS

LIST OF FIGURES

Figure **Page**

LIST OF ABBREVIATIONS

ASR	Aperiodic Stochastic Resonance
CR	Cognitive Radio
DWVD	Discrete-time Wigner Ville Distribution
EQ	Equilibrium Point
FPE	Fokker-Planck Equation
FLOC	Fractional Lower Order Covariance
FLOM	Fractional Lower Order Moment
FLOPPS	Fractional Lower Order Pseudo Power Spectrum
FLOS	Fractional Lower Order Statics
FLOWVD	Fractional Lower Order Wigner Ville Distribution
FLOPWVD	Fractional Lower Order Polynomial Wigner Ville Distribution
MR	Mean Residence Time
PLC	Predicted Limit Cycle
PPS	Pseudo Power Spectrum
QTFR	Quadratic Time Frequency Representation
SMR	Stochastic Multi-Resonance
SNR	Signal-to-Noise Ratio
SPA	Spectral Power Amplification
SR	Stochastic Resonance
SSR	Suprathreshold Stochastic Resonance
TFR	Time Frequency Representation
WVD	Wigner Ville Distribution

CHAPTER 1

INTRODUCTION

In general, noise is considered to have negative effects on the performance of any system. In order to suppress or eliminate noise from system, filtering and feedback compensation are carried out. However, over the last thirty years the studies have shown the positive effects of noise. In nonlinear dynamical systems, the presence of an optimal amount of noise provides a better system response than in the absence of noise such as enhancement of the degree of coherence (Gang, Ditzinger et al. 1993), amplification of the weak periodic signals (Jung and Hänggi 1991) and increase of signal-to-noise ratio (SNR) (Benzi, Sutera et al. 1981). This phenomenon is called as stochastic resonance (SR) and originally introduced to explain the periodic climatic changes of the Earth's ice ages (Benzi, Sutera et al. 1981).

The global climate is modeled as a symmetric double well potential by (Benzi, Sutera et al. 1981). The well has two states in which one state represents the Earth's temperature in the ice regime while the other state is in the warm regime. According to the climate records, the period for Earth's climate switching between ice ages and warmer regime is around 100.000 years. This time coincides with the period of the eccentricity of the Earth's orbit. However it is considered that the combination of stochastic perturbations along with the changing eccentricity cause such dramatic changes in climate rather than the eccentricity alone. The tiny oscillations of the Earth's orbital eccentricity are considered as a periodic forcing signal and short-term climate fluctuations, due to the annual fluctuations in solar radiation, are modeled as the Gaussian white noise and the transition from ice climate to warm climate perturbed by the earth's orbital eccentricity have been induced in the presence of a non-zero noise level of the atmosphere (Benzi, Parisi et al. 1982; Benzi, Parisi et al. 1983).

Stochastic resonance has evolved from a very specific context but later on it has been observed in many fields of science such as physics (Gammaitoni, Hänggi et al. 1998; Anishchenko, Neiman et al. 1999), electronic circuits (Anishchenko and Safonova 1992; Anishchenko, Neiman et al. 1993) (Gomes, Mirasso et al. 2003) (Korneta, Gomes et al. 2006), chemical reactions (Leonard and Reichl 1994), biological

systems (Moss, Ward et al. 2004), biomedical applications (Collins, Imhoff et al. 1996) (Richardson, Imhoff et al. 1998) (Kurita, Shinohara et al. 2011) (Morse and Evans 1996) telecommunication (He, Lin et al. 2010).

Usually stochastic resonance is observed when a sub-threshold signal (the signal below a specified threshold) is subjected to an optimal amount of noise. In such systems when the input signal is supra-threshold (the signal above a specified threshold) then the addition of noise will not have any beneficial effect on the systems output. However, studies have shown that SR can also occur when the input forcing is supra-threshold or aperiodic signal. The term aperiodic SR (ASR) (Collins, Chow et al. 1995) and supra-threshold SR (SSR) (Stocks 2000; McDonnell, Stocks et al. 2008) has been defined to describe this type of behaviors.

The characteristics of SR such as the spectral power amplification (SPA), the signal-to-noise ratio (SNR) or cross-correlation between the input and output signals measure have a maximum at an optimal amount of noise. For sub-threshold periodic signals, the peak value corresponding to the input signal frequency in the output power spectrum enhances with the addition of an optimal amount noise. This enhancement in the presence of noise reveals the effect of SR. Since the SNR is not appropriate method for aperiodic signals to quantify the SR, the correlation between the input and output signals has been proposed to characterize the system's response (Collins, Chow et al. 1995). Other measures of SR, based on residence time distribution have been introduced in (Gammaitoni, Marchesoni et al. 1995) .

1.1. Outline of the Thesis

The main structure of this thesis is divided into six parts. The first chapter gives a general overview of stochastic resonance introducing the motivation and applications. Chapter 2 provides the detailed study of SR beginning with its physical background. The α-stable distributions and the spectral representations in impulsive environments are explained in Chapter 3. In Chapter 4, the Chua's circuit driven α-stable noise and the harmonic balance method used to analyze the dynamics of the model theoretically are introduced. The simulation results to observe the effect of SR in the framework of spectral power amplification and the mean residence times under the various noise parameters are presented in Chapter 5. The simulations will be implemented by using

computational software program Matlab®. Finally, Chapter 6 concludes with the main results of the thesis and proposes the future work.

1.2. Motivation and Applications

There have been increasingly important applications of SR in various fields. According to the Web of Science, the total number of publications with the topic of stochastic resonance is around 5000 over a period of a thirty years and physics, engineering, mathematics, computer science and neurosciences are the first-five subject areas. Even there are 54 papers focused on stochastic resonance in telecommunication. The works related to stochastic resonance show that how stochastic resonance is still an interesting subject to work on. Some of many interesting research results are briefly explained below:

The first demonstration of stochastic resonance in biology utilized the mechanoreceptors, sensory hairs, located on the tail fan of the crayfish. These receptors evolved for the purpose of long-range detection of predators are sensitive to the water vibrations and pressure waves caused by the prey or enemies. The presence of an optimal amount of noise may enhance the sensitivity of receptors to detect weak signals of the crayfish predator's while it's still far enough away and enable to crayfish escape (Douglass, Wilkens et al. 1993) (Bahar and Moss 2003).

The noise-enhanced feeding behaviour of the paddlefish (*Polyodon spathula*) has been investigated by (Russell, Wilkens et al. 1999). Paddlefish uses electroreceptors to detect its feed Daphnia. Electroreceptors in paddlefish form a passive sensory system to detect electrical signals from external sources such as swarms of Daphnia. A randomly varying electrical field was applied in the environment of paddlefish. The amplitude of noise has been varied and the strike locations where the paddlefish catch the prey were measured. It was found that with the optimal amount of noise the distance that the paddlefish can sense and capture the prey will be increased. For higher noise levels, the sensitivity of the electroreceptors gradually decreases again, resulting in almost no detection (Russell, Wilkens et al. 1999; Freund, Schimansky-Geier et al. 2002).

Stochastic resonance has been also observed in biomedical applications. The human tactile sensation has been observed in (Collins, Chow et al. 1995). A non-zero

level of random vibration added to the stimulator enhances the detection of weak touches on the observers' fingers (Collins, Imhoff et al. 1996). Direct electrical stimulation of the touch receptors with a randomly varying electrical current added to a touch stimulus resulted in SR for tactile sensation (Richardson, Imhoff et al. 1998).

Medical devices such as vibrating gel-based insoles have been created based on the effect of stochastic resonance to improve the balance of elderly people and nerve sensitivity of patients with diabetic neuropathy or stroke. This enhancement of sensitivity in the foot nerves potentially reduces the risk of fall and sway (Priplata, Niemi et al. 2003; Priplata, Patritti et al. 2006) .

The wearable orthopaedic device, named sensorimotor enhancer, has been designed to enhance one's sense of touch through a small vibrator attached to the side of the fingertip (Kurita, Shinohara et al. 2011) in which the experimental results in various sensing ability tests have confirmed that the application of appropriate vibrations enhanced the tactile sensitivity of the fingertip. This special glove can hold objects using less force, sense filaments at lighter filaments and assist people with medical conditions that reduce their sense of touch.

The effective auditory noise significantly increased tactile sensations of the finger, decreased luminance and contrast visual thresholds (Lugo, Doti et al. 2008)

The application of stochastic resonance for efficient encoding of auditory information has been used in cochlear implants (Morse and Evans 1996; Stocks, Allingham et al. 2002). The hair cells of the inner ear normally convert mechanical sound vibrations into electrical signals. Hair cells can be severely damaged and the loss of hair cells causes hearing loss. Since an acoustic stimulus cannot produce neural activities in the loss of hair cells the amplification of sounds by a hearing aid will not be helpful. Cochlear implants which are surgically inserted into the ear restore hearing to the profoundly deaf people. They replace the function of the hair cells and work by direct electrical stimulation of the cochlear nerve. The addition of an optimum amount of noise to cochlear implant signals can improve the detection of low amplitude signals at the threshold level and the discrimination of smaller frequency differences at the supra-threshold level (Morse and Roper 2000). The addition of noise providing randomness to the output of cochlear implant electrical signals also enables to stimulate nerve fibres in a natural way.

SSR has been investigated to improve speech comprehension in patients with cochlear implants in (Stocks, Allingham et al. 2002).

(Kay, Michels et al. 2006) has presented the occurrence of SR in a suboptimal detector. The enhancement of detection performance can be achieved by adding noise to the data under certain conditions. The criterion for the detection performance has been chosen as the probability of a decision error and the probability density function of this optimal noise has been determined as a Dirac delta function for the minimum probability of a decision error in which the optimal additive noise corresponds to a constant signal (Kay, Michels et al. 2006).

A spectrum-sensing method for cognitive radio (CR) based on SR has been proposed in (He, Lin et al. 2010) in which the performance of secondary users (SU) to detect weak signals of primary signals (PU), especially under low SNR conditions, can be enhanced and the spectrum utility in CR networks can be improved.

The effect of noise on the memory elements such as memristors, memcapacitors and meminductors have been investigated in (Stotland and Di Ventra 2011). In their study, a physical model of memory resistor has been used to illustrate the phenomenon of SR to show that under specific conditions on the noise intensity the memory can actually be enhanced.

(Marks, Thompson et al. 2002) has studied the enhancement of the appearance of an image using stochastic resonance.

Stochastic resonance can be used to improve the detection of small features such as lesions or tumours in mammograms (Peng, Chen et al. 2009)

The effects of background white noise on the memory performance of inattentive school children have been investigated in (Söderlund, Sikström et al. 2010)

1.3. Objective of the Thesis

According to literature, noise-added systems and in particular stochastic resonance are still an interesting subject to work on. Almost all studies related to the stochastic resonance phenomenon in the chaotic systems assume the noise is Gaussian hence has a finite variance. Instead, in this thesis we consider non-Gaussian noise case and investigate the stochastic resonance in a Chua's circuit subjected to alpha-stable

noise which has better approximation to a real-world signal than Gaussian distribution in certain cases.

The aims of this thesis can be listed as follows:

i. To determine the threshold amplitude value of periodic input forcing as a function of its frequency,
ii. to study the amplification of the sub-threshold input periodic signal as a function of the noise intensity to observe the effect of SR and analyze the response of model by varying alpha-stable parameters,
iii. to determine the mean residence time in an attractor under the various noise parameters to investigate the change of the average lifetime of a trajectory in an attractor.

CHAPTER 2

STOCHASTIC RESONANCE

In nonlinear systems the response of a sub-threshold periodic input signal can be improved by the presence of a particular amount of noise. This sub-threshold signal is too weak to switch between states; however threshold crossings can occur with the addition of noise to the system.

SR has been observed in a variety of physical systems and even in biological sensory neurons, suggesting that it may play an important role in such systems. Experiments have demonstrated that stochastic resonance occurs in sensory systems such as human tactile sensation (Collins, Imhoff et al. 1996), human visual perception and human vision (Lugo, Doti et al. 2008). The existence of stochastic resonance has been investigated also at the level of vital animal behaviour such as mechanoreceptors in crayfish (Douglass, Wilkens et al. 1993) and the animal feeding behavior (Russell, Wilkens et al. 1999).

SR can be observed in bistable systems as well as chaotic systems (Anishchenko and Safonova 1992). SR phenomenon has been also investigated in Chua's circuit driven by Gaussian noise and either amplitude-modulated or frequency modulated signal (Anishchenko and Safonova 1994). SR in the presence of multiplicative noise and the effect of oscillations in a symmetric double well potential driven by a sub-threshold periodic forcing has been demonstrated in (Gammaitoni, Hänggi et al. 1998). Although traditional SR requires the weak and periodic signal, aperiodic (Collins, Chow et al. 1995) (Barbay, Giacomelli et al. 2000) and suprathreshold signals (Stocks 2000; McDonnell, Stocks et al. 2008) can also be the input of certain SR systems. High frequency SR in Chua's circuit and the effect of SR in a Chua's circuit perturbed by Gaussian noise has been studied experimentally in (Gomes, Mirasso et al. 2003) and (Korneta, Gomes et al. 2006), respectively. The most common and extensively studied noise is the additive zero-mean white Gaussian noise however it can be non-Gaussian noise or chaotic signals. The investigation of the double-well potential model driven by the α-stable and Lèvy type noise have shown the presence of stochastic resonance in (Dybiec and Gudowska-Nowak 2006) (Dybiec and Gudowska-Nowak 2009).

The other effect is coherence resonance in which the optimum response (in the sense of optimal periodicity) occurs for a non-zero value of noise but in the absence of periodic forcing (Palenzuela, Toral et al. 2001).

In (Kosko and Mitaim 2001) (Kosko and Mitaim 2003) a forbidden interval has been defined in the studies of stochastic resonance in threshold based systems. The forbidden interval theorem gives both necessary and sufficient conditions for the SR effect. The forbidden interval is defined as the region $[\theta - A,\ \theta + A]$ where θ is the threshold value and binary signal takes values from $\{-A,\ A\}$. According to forbidden interval theorem, SR will occur for all finite variance noise distributions if and only if the mean of the noise is outside the forbidden interval and for all infinite variance stable noise distributions, if and only if the location parameter of the noise is outside the forbidden interval. Although in SR studies the noise is usually assumed to be finite variance such as Gaussian, (Kosko and Mitaim 2001) concludes that SR occurs also for impulsive noise.

2.1. Physical Background

The physical mechanism of Stochastic Resonance can be simply explained by investigating the model of an over-damped bistable system shown as in Figure 2.1.

The potential of the particle at any position x is given by *V(x)*

$$V(x) = -\frac{a}{2}x^2 + \frac{b}{4}x^4 \tag{2.1}$$

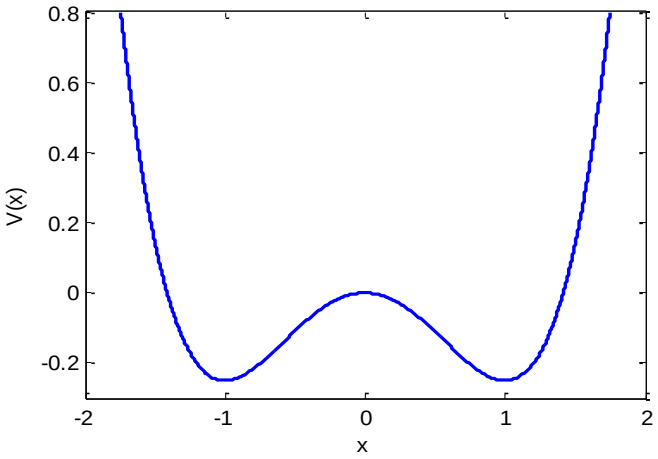

Figure 2.1. The bistable potential with the parameters $a = b = 1$

The well has two stable states and the minima of *V(x)* are located at $\pm x_m$ where $x_m = (a/b)^{1/2}$ and unstable one at $x = 0$. In the absence of external forcing signal, the particle will stay in one of the equilibrium states at the bottom of the wells.

The motion of a Brownian particle in a double well potential *V(x)* perturbed by an external periodic forcing and noise is described as (Gammaitoni, Hänggi et al. 1998)

$$\frac{dx(t)}{dt} = -\frac{dV(x)}{dx} + A_0 \sin(w_0 t) + \xi(t) \tag{2.2}$$

where $x(t)$ is the position of particle and $A_0 \cos(w_0 t)$ is the deterministic forcing signal acting on the system.

$\xi(t)$ indicates white Gaussian noise, $< \xi(t)\, \xi(t+\tau) >= 2D\delta(t)$, with intensity *D*.

The time-dependent bistable potential shown as in Figure 2.2 is described as

$$V(x,t) = \mathrm{V}(x) - A_0\, x \sin(w_0 t) \tag{2.3}$$

where A_0 and w_0 are the amplitude and frequency of the periodic signal respectively.

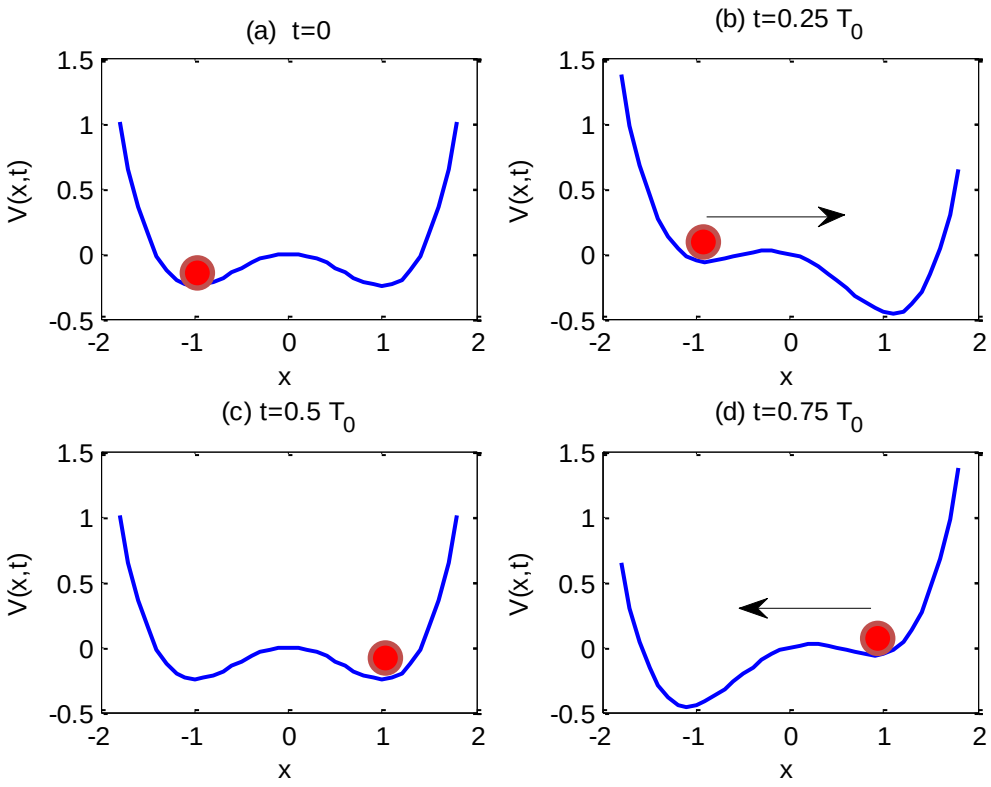

Figure 2.2. The cyclic variation of bistable potential with periodic modulation.

If a weak periodic force is applied to the system, the potential well is tilted asymmetrically up (Figure 2.2 (b)) and down one period later (Figure 2.2 (d)). The raising and lowering the wells continues periodically, as shown in Figure 2.2.

Since the periodic forcing is too weak there is no crossing from one potential well to the other one. The particle will oscillate in one of the wells but will not hop to the other. However, a sufficiently strong level of noise can cause the particle to overcome the energy barrier and move into the deeper potential well. At the next half cycle the potential well is tilted again so noise can again push the particle into the adjacent well. The arrows shown in Figure 2.2 indicate the possible direction of crossing the well in the presence of noise.

In the absence of periodic forcing the particle fluctuates around one of the equilibrium points of the potential wells. With the addition noise, the particle switches between two wells with a mean rate (frequency) given by the Kramer's rate r_K.

The Kramer's rate is defined as the characteristic escape rate from a stable state of the potential

$$r_K = \frac{1}{2\pi}[V(x_{max})''|V(x_{min})'']^{1/2} exp\left(-\frac{\Delta V}{D}\right) \quad (2.4)$$

where $V'' \triangleq \frac{d^2V(x)}{dx^2}$, x_{max} and x_{min} are the coordinates of the potential maximum and minimum, respectively. ΔV is the potential barrier and D is the noise intensity.

The Kramer's rate depends on the noise intensity. The reciprocal of the Kramer's rate refers to the periodicity or mean residence time in one of the potential well and given as

$$T_k(D) = 1/r_k(D) \quad (2.5)$$

When a weak periodic forcing is applied to the system noise induced switching between the potential wells can become synchronized with the weak periodic forcing. The synchronization between the input signal and noise occurs when the mean residence time satisfies the time-scale matching requirement

$$T_\Omega = 2T_k(D) \quad (2.6)$$

where T_Ω is the period of the input periodic forcing term.

The Kramer's rate also determines the probabilities of switching events.

2.2. Characteristic of Stochastic Resonance

The quantitative characteristics of Stochastic Resonance depend on the physical mechanism of the system, the kind of nonlinear system driven, the character of the input signal and the noise. These characteristics such as spectral power amplification (SPA) (Jung and Hänggi 1991), signal-to-noise ratio (SNR) (Benzi, Sutera et al. 1981), mutual information (Bulsara and Zador 1996), correlation coefficient (Collins, Chow et al. 1995) and residence-time distributions (Gammaitoni, Hänggi et al. 1998) can be calculated analytically and numerically, or measured in physical systems.

2.2.1. The Spectral Power Amplification (SPA)

Spectral power amplification is defined by the ratio of the power stored in the response of system at the frequency of input signal to the the power of the input forcing signal at the frequency of input signal (Jung and Hänggi 1991).

$$\eta = \frac{P_{out}(w_0)}{P_{in}(w_0)} \tag{2.7}$$

where $P_{out}(w_0)$ and $P_{in}(w_0)$ are the power spectrums of the output and input signals calculated at the frequency w_0 of the input signal, respectively.

2.2.2. The Signal-to-Noise Ratio (SNR)

The signal-to-noise ratio is defined as the ratio of the output signal power at the input signal frequency to the background noise power spectrum (Anishchenko, Neiman et al. 1999):

$$SNR = \frac{1}{S_{x,x}^{(0)}(w_0)} 2 \int_{\Omega-\Delta w}^{\Omega+\Delta w} S_{x,x}(w)dw \tag{2.8}$$

$\int_{w_0-\Delta w}^{w_0+\Delta w} S_{x,x}(w)dw$ indicates the output signal power and the noise background $S_{x,x}^{(0)}(w)$ is calculated at the frequency of the input signal, $w = w_0$. The frequency range corresponds to $w_0 \pm \Delta w$ and Δw is the frequency resolution.

2.2.3. The Residence-time Distribution

The output of bistable system can be converted into a two-state dynamics by setting two crossing levels, for instance

$$x(t) = \begin{cases} +c, & x(t) > x_{threshold} \\ -c, & x(t) < -x_{threshold} \end{cases} \tag{2.9}$$

where c is a constant and $x_{threshold}$ is the crossing threshold value. In the two-state dynamics the system resides at any time in either one of the two states.

The residence time T_r is defined as the time the particle spends in one state. The distribution of the residence time decays exponentially of the following form

$$\rho(T) = r_k exp(-r_k T) \tag{2.10}$$

where $\rho(T)$ indicates the residence time distribution function.

The area under the peak of the residence time distribution corresponding to the input forcing signal frequency goes through a maximum as a function of noise intensity.

The switching time T_s is the time between two consecutive arrivals to one of the states. The probability distribution of switching times is usually determined for the stochastic resonance phenomenon in biological systems. It corresponds e.g. to an inter-spike interval histogram recorded from real periodically forced sensory neurons (Longtin 1993).

2.3. Response to a Weak Signal

The theoretical analysis of stochastic resonance systems is often very difficult due to the complexity of the systems. Approximation models have been adopted in some cases. Some of them for the theoretical analysis are two-state model, Fokker-Planck equation and linear-response theory.

The dynamical equation of the model of over-damped oscillator given in Equation 2.2 is rewritten as

$$\dot{x} = x - x^3 + A\, cos(\Omega t + \varphi_0) + \sqrt{2D}\xi(t) \tag{2.11}$$

The corresponding Fokker-Planck equation (FPE) for the transition probability density $p(x, t|x_0, t_0; \varphi_0)$ gives the evolution of probability density function (*pdf*) in time (Anishchenko, Neiman et al. 1999):

$$\frac{\partial p}{\partial t} = -\frac{\partial}{\partial x}\{[x - x^3 + A\,cos(\Omega t + \varphi_0)]p\} + D\frac{\partial^2 p}{\partial x^2} \tag{2.12}$$

The equation can be rewritten in the form

$$\frac{\partial p}{\partial t} = [\mathcal{L}_0 + \mathcal{L}_{ext}]\,p \tag{2.13}$$

where $\mathcal{L}_0$ is the unperturbed Fokker-Planck operator ($A = 0$) and $\mathcal{L}_{ext}(t)$ represents the periodic perturbation:

$$\mathcal{L}_0 = -\frac{\partial}{\partial x}(x - x^3) + D\frac{\partial^2}{\partial x^2}\ , \tag{2.14}$$

$$\mathcal{L}_{ext}(t) = -A\,cos(\Omega t + \varphi_0)\,\partial/\partial x\ . \tag{2.15}$$

The probability in the asymptotic limit $t_0 \to -\infty$ is expanded into Fourier series

$$p_{asy}(x, t; \varphi_0) = \sum_{n=-\infty}^{\infty} p_n(x)\exp[i(n\Omega t + \varphi_0)] \tag{2.16}$$

The nonlinear response of the stochastic system to the harmonic force can be found in (Anishchenko, Neiman et al. 1999):

$$\langle x(t)\rangle_{asy} = \sum_{n=-\infty}^{\infty} M_n \exp[i(n\Omega t + \varphi_0)] \tag{2.17}$$

where the M_n are the complex amplitudes that depend on the noise intensity *D*, the signal frequency Ω, and the amplitude *A*.

The spectral power amplification η is defined as (Jung and Hänggi 1991)

$$\eta = \left(\frac{2|M_1|}{A}\right)^2 \tag{2.18}$$

2.4. Two-State Theory

The master equation for the probabilities $n_{\pm}(t)$ of residing in one of the two states $\pm x_m$ is defined as (Anishchenko, Neiman et al. 1999)

$$\dot{n_{\pm}}(t) = -W_{\mp}(t)n_{\pm} + W_{\pm}(t) \tag{2.19}$$

where $W_{\pm}$ and $W_{\mp}$ are the transition rates from one state to another.

Using the normalization condition $n_{\pm}(t) + n_{\mp} = 1$, Equation 2.19 can be rewritten as the form

$$\dot{n_{\pm}}(t) = -\left[W_{\pm}(t)n_{\pm} + W_{\mp}(t)\right]n_{\pm} + W_{\pm}(t) \tag{2.20}$$

The solution of this rate equation can be found analytically for a given $W_{\pm}(t)$. The following form for the transition probability densities $W_{\pm}(t)$ is proposed by (McNamara and Wiesenfeld 1989)

$$W_{\pm}(t) = r_K \exp\left[\pm\frac{Ax_m}{D}\cos(\Omega t)\right] \tag{2.21}$$

where r_K is the Kramer's rate.

It is clear from Equation 2.21 in the absence of external force signal $(A = 0)$ the probability densities of switching $W_{\pm}(t)$ are equal to the Kramer's rate r_K.

Any statistical characteristics of the process can be evaluated by conditional probabilities. Using the solution of Equation 2.20 the conditional probability is determined as (Anishchenko, Neiman et al. 1999)

$$p(x,t|x_0,t_0) = n_{\pm}(t)\delta(x - x_m) + n_{\mp}(t)\delta(x + x_m) \tag{2.22}$$

The mean value obtained by averaging the $x(t)$ with initial conditions $x_0 = x(t_0)$ over the ensemble of the noise realizations is given by the following expression

$$\langle x(t)|x_0,t_0\rangle = \int xp(x,t|x_0,t_0)dx \tag{2.23}$$

The asymptotic limit $(t \to -\infty)$ is obtained in (Anishchenko, Neiman et al. 1999)

$$\langle x(t)\rangle_{as} = \lim_{t_0\to-\infty}\langle x(t)|x_0,t_0\rangle = A_1(D)cos[\Omega t + \psi(D)] \tag{2.24}$$

with the amplitude $A_1(D)$ and the phase lag $\psi(D)$.

$$A_1(D) = \frac{A{x_0}^2}{D}\frac{2r_K}{\sqrt{4{r_K}^2 + \Omega^2}} \tag{2.25}$$

$$\psi(D) = arctan\left(\frac{\Omega}{2r_K}\right) \tag{2.26}$$

The autocorrelation function is defined as

$$\langle x(t+\tau)x(t)|x_0,t_0\rangle = \int\int xy\, p(x,t+\tau|y,t)p(y,t|x_0,t_0)dxdy \tag{2.27}$$

The phase-averaged power spectral density $S(w)$ is defined as

$$S(w) = \int_{-\infty}^{\infty} e^{-iw\tau}\langle\langle x(t+\tau)x(\tau)\rangle\rangle\, d\tau \tag{2.28}$$

where the inner brackets denote the ensemble average over the realizations of the noise and outer brackets indicate the average over the input initial phase ψ in (2.26).

The spectral power amplification (SPA) is determined in (Anishchenko, Neiman et al. 1999)

$$\eta = \frac{4{r_K}^2{x_m}^4}{D^2(4{r_K}^2 + \Omega^2)} \tag{2.29}$$

And the signal-to-noise ratio for the two state model

$$SNR = \pi\left(\frac{Ax_m}{D}\right)^2 r_K \tag{2.30}$$

From Equation 2.30 it is seen that a single maximum as a function of the noise intensity *D* occurs.

CHAPTER 3

ALPHA-STABLE DISTRIBUTIONS

The Gaussian distribution have played an important role in signal processing. This is because it is characterized completely by the first moment and the second moment of the distribution and it often leads to reduction in the analytical complexity of a system and ensures analytical solution in most cases.

However, many physical phenomena are non-Gaussian and show a very impulsive (heavy-tailed) distribution. Gaussian distribution is inadequate for modeling such heavy-tailed and asymmetric densities. Stable distributions, also sometimes referred to as the α-stable distributions, have received a growing interest due to the ability to model signals of this impulsive nature. This type of a signal tends to produce outliers. These distributions share same characteristics with the Gaussian distribution such as the stability property and central limit theorems. The parameter α, is the characteristic exponent that varies over $0 \leq \alpha < 2$. In fact, the Gaussian distribution is a special case of the alpha-stable distribution ($\alpha = 2$).

Stable distributions have found numerous applications in various fields such as economics, hydrology, physics, biology and telecommunication. The most important application of the stable distribution in signal processing is in the area of impulsive noise modeling.

The signal detection method in non-Gaussian environment can be found in (Chiang and Nikias 1990; Tsihrintzis and Nikias 1995). The frequency estimation of the sinusoidal signals in α-stable noise environment has been analyzed in (Altınkaya, Deliç et al. 2002). The methods for parameter estimation (Ma and Nikias 1995; Tsihrintzis and Nikias 1996) and blind channel identification with the non-Gaussian input of parameters have been introduced in (Ma and Nikias 1995). Parameter estimation of skewed α-stable distributions has been presented in (Kuruoglu 2001).

Statistical moments give information on the characteristics of signals. Although the whole spectrum of statistical moments range from order 0 to order ∞ shown as in Figure 3.1 (Nikias and Shao 1995), the traditional signal processing methods utilize only the second-order moments. However, signal processing methods based on α-stable

distributions have no finite first-or higher order moments for $0 < \alpha \leq 1$ and , they have only the first moments for $1 < \alpha < 2$ and all the fractional lower order moments (FLOMs) of order p where $p < \alpha$.

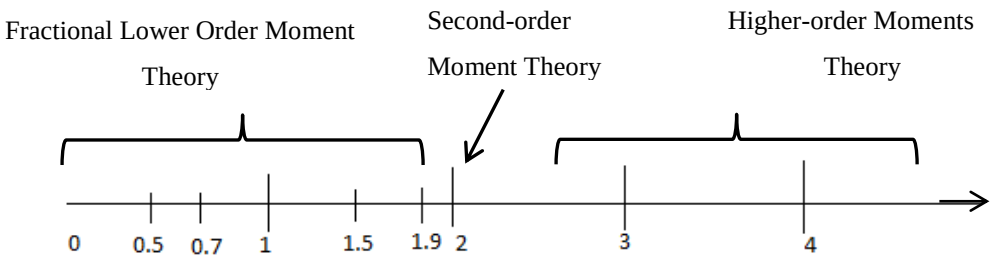

Figure 3.1. Statistical moments
(Source: Nikias and Shao 1995)

3.1. Alpha Stable Random Variables

Two of the most important properties of the stable distribution are the stability property and the Generalized Central Limit theorem.

The stability property is defined as a characteristic of the stable distribution. The sum of independent, identically distributed (i.i.d.) stable random variables will retain the shape of the original distribution.

The generalized central limit theorem states that the sum of many random variables with identical distributions, not necessarily with finite variances, converges to a stable distribution.

Definition 3.1.1 (Samorodnitsky, 1994): A random variable X is said to have a stable distribution if for any positive numbers A and B, there is a positive number C and a real number D such that

$$AX_1 + BX_2 \overset{d}{=} CX + D \tag{3.1}$$

where X_1 and X_2 are independent realizations of X, and $\overset{d}{=}$ denotes equality in distribution.

Definition 3.1.2 (Samorodnitsky1994): A random variable X is said to have a stable distribution if for any $n \geq 2$, there is a positive number C_n and a real number D_n such that

$$X_1 + X_2 + \cdots + X_n = C_n X + D_n \tag{3.2}$$

where $X_1, X_2, \ldots, X_n$ are identical independent distributions (i.i.d).

Definition 3.1.3 (Samorodnitsky 1994): A random variable X is said to have stable distribution if there are parameters $0 < \alpha \leq 2$, $\sigma \geq 0$, $-1 \leq \beta \leq 1$, and $-\infty < \mu < \infty$ such that its characteristic function can be described as:

$$\varphi(w) = \begin{cases} \exp\left\{-\sigma^{\alpha}|w|^{\alpha}\left(1 - i\beta(\text{sign } w)tan\frac{\pi\alpha}{2}\right) + i\mu w\right\} & \text{if } \alpha \neq 1 \\ \exp\left\{-\sigma^{\alpha}|w|\ \left(1 + i\beta(\text{sign } w)tan\frac{\pi\alpha}{2}\right) + i\mu w\right\} & \text{if } \alpha = 1 \end{cases} \tag{3.3}$$

where

$$sign(w) = \begin{cases} 1 & \text{if } w > 0 \\ 0 & \text{if } w = 0 \\ -1 & \text{if } w < 0 \end{cases}. \tag{3.4}$$

A stable distribution is characterized by four parameters: α, β, μ, σ and denoted by $S_{\alpha}(\sigma, \beta, \mu)$: The characteristic exponent denoted by α measures the thickness of the tails of the distribution and show the impulsiveness of the signal. A stable distribution with characteristic exponent α is called α-stable. The skewness parameter β describes the symmetry and μ is a location parameter, it is the mean when$1 < \alpha \leq 2$ and the median when $0 < \alpha < 1$. The scaling σ or the dispersion parameter $\gamma = \sigma^{\alpha}$ determines the spread of distribution around its location parameter μ in the same way that the variance of a Gaussian distribution determines the spread around the mean.

The α-stable distribution is symmetric when $\beta = 0$ and represented by $X \sim S\alpha S$. "~" refers to "has distribution".

For $S\alpha S$ distributions, the location parameter μ is the mean when $1 < \mu \leq 2$ and the median when $0 < \mu < 1$.

The characteristic function of the $S\alpha S$ distribution is in the form

$$\varphi(w) = exp\{jw\mu - \gamma|w|^{\alpha}\} \tag{3.5}$$

In this case, the characteristic function of a $S\alpha S$ distribution is determined only by the characteristic exponent and dispersion,

$$\varphi(w) = exp\{-\gamma|w|^{\alpha}\} \tag{3.6}$$

where $0 < \alpha \leq 2$ and $\gamma > 0$

A $S\alpha S$ distribution is standard if $\gamma = 1$.

The probability density function (*pdf*) of α-stable distributions can be found by taking the conjugate of inverse Fourier transform of the characteristic function (Shanmugan and Breipohl 1988).

$$f(x) = \frac{1}{2\pi}\int_{-\infty}^{\infty} \varphi(w)e^{-iwx}\,dw \tag{3.7}$$

However, with few exceptions, there is no closed form expression for the probability density function. The exceptions are:

I. Gaussian distribution, $S_2(\sigma, \beta, \mu)$

$$f(x) = \frac{1}{2\sigma\sqrt{\pi}} exp\left\{-\frac{(x-\mu)^2}{4\sigma^2}\right\} \tag{3.8}$$

II. Cauchy distribution , $S_1(\sigma, 0, \mu)$

$$f(x) = \frac{2\sigma}{\pi((x-\mu)^2 + 4\sigma^2)} \tag{3.9}$$

III. Lévy distribution, $S_{1/2}(\sigma, 1, \mu)$

$$f(x) = \frac{\sigma}{\sqrt{2\pi(x-\mu)^3}} exp(-\frac{\sigma}{2(x-\mu)}) \tag{3.10}$$

3.1.1. Properties of α-Stable Distributions

The following properties shown below are the basic properties of stable distributions given by (Samorodnitsky and Taqqu):

Property 3.1.1.1 Let X_1 and X_2 be independent random variables with $X_1 \sim S_\alpha(\sigma_1, \beta_1, \mu_1)$ and $X_2 \sim S_\alpha(\sigma_2, \beta_2, \mu_2)$ then $X_1 + X_2 \sim S_\alpha(\sigma, \beta, \mu)$ with

$$\sigma = ({\sigma_1}^\alpha + {\sigma_2}^\alpha)^{1/\alpha}, \qquad \beta = \frac{\beta_1 {\sigma_1}^\alpha + \beta_2 {\sigma_2}^\alpha}{{\sigma_1}^\alpha + {\sigma_2}^\alpha}, \qquad \mu = \mu_1 + \mu_2 \tag{3.11}$$

Property 3.1.1.2 Let X be a random variable with location μ, $X \sim S_\alpha(\sigma, \beta, \mu)$ and c be a real constant then $X + c \sim S_\alpha(\sigma, \beta, \mu + c)$.

Property 3.1.1.3 Let $X \sim S_\alpha(\sigma, \beta, \mu)$ and c be a non-zero real constant then

$$cX \sim S_\alpha(|c|\sigma, \text{sign}(c)\beta, c\mu) \qquad \text{if } \alpha \neq 1 \tag{3.12}$$

$$cX \sim S_\alpha\left(|c|\sigma, \text{sign}(c)\beta, c\mu - \frac{2}{\pi}c(\ln|c|\sigma\beta)\right) \qquad \text{if} \quad \alpha=1 \tag{3.13}$$

For any $0 < \alpha < 2$,

$$X \sim S_\alpha(\sigma, \beta, \mu) \Leftrightarrow -X \sim S_\alpha(\sigma, -\beta, \mu) \tag{3.14}$$

Property 3.1.1.4 $X \sim S_\alpha(\sigma, \beta, \mu)$ is symmetric about μ if and only if $\beta = 0$.

Property 3.1.1.5 Let $X \sim S_\alpha(\sigma, \beta, \mu)$ with $0 < \alpha < 2$ then

$$E\{|X|^p\} < \infty \qquad \text{for any } \ 0 < p < \alpha \ , \tag{3.15}$$

This implies that α-stable distributions with $\alpha < 2$ have infinite second and higher order moments and if $\alpha = 2$ then

$$E|X|^p < \infty \qquad \text{for all } \ p \geq 0 \, . \tag{3.16}$$

If $\alpha \leq 1$ then even first-order moment $E\{X\} = \infty$.

$$E\{|X|^p\} = \infty \qquad \text{for any } \ p \geq \alpha \ . \tag{3.17}$$

3.1.2. Generation of Stable Random Variables

For any symmetric α-stable random variables $X \sim S_\alpha(1,0,0)$ where $\alpha \in (0,2]$ can be generated applying the following transformation.

$$X = \frac{sin(\alpha V)}{\{cos(V)\}^{1/\alpha}} \times \left\{\frac{cos(V - \alpha V)}{W}\right\}^{(1-\alpha)/\alpha} \tag{3.18}$$

where V is a random variable uniformly distributed on $(-\pi/2\,, \pi/2)$ and W is an exponential random variable with mean one (Janicki and Weron 1994).

The following algorithm provides a good technique of computer simulation of skewed stable random variables (Janicki and Weron 1994).

$$Y \sim S_\alpha(1, \beta, 0) \text{ with } \alpha \in (0,1) \cup (1,2] \text{ and } \beta \in [-1,1] \tag{3.19}$$

$$Y = D_{\alpha,\beta} \times \frac{sin\left(\alpha\left(V + C_{\alpha,\beta}\right)\right)}{\{cos(V)\}^{\frac{1}{\alpha}}} \times \left\{\frac{cos\left(V - \alpha\left(V + C_{\alpha,\beta}\right)\right)}{W}\right\}^{\frac{1-\alpha}{\alpha}} \tag{3.20}$$

$$C_{\alpha,\beta} = \frac{arc\ tan\left(\beta\ tan(\pi\alpha/2)\right)}{1 - |1 - \alpha|} \tag{3.21}$$

$$D_{\alpha,\beta} = \left[cos\left(arc\ tan\left(\beta\ tan(\pi\alpha/2)\right)\right)\right]^{1/\alpha} \tag{3.22}$$

where V is a random variable uniformly distributed on $(-\pi/2, \pi/2)$ and W is an exponential random variable with mean one.

Using a numerical approximation of the formula in Equation 3.7 α-stable densities can be constructed in the general case. Figures 3.2- 3.6 present the result of computer simulations of such densities for different values of α, β, σ parameters and also show how α-stable density functions illustrated as $f(x)$ depend on parameters. The location parameter μ is set to zero for all case.

It is shown as in Figure 3.2 that the distribution is highly impulsive with small characteristic exponent α. Figure 3.3 shows the dependence of density on scaling parameter σ. When the skewness parameter β is positive, the distribution is skewed to the right when β is negative, it is skewed to the left shown as in Figures 3.4-3.5. The decrease of parameter α leads to the increase of non-symmetric behavior of distributions in skewed distributions (i.e., β is different from 0) shown as in Figure 3.6-3.7.

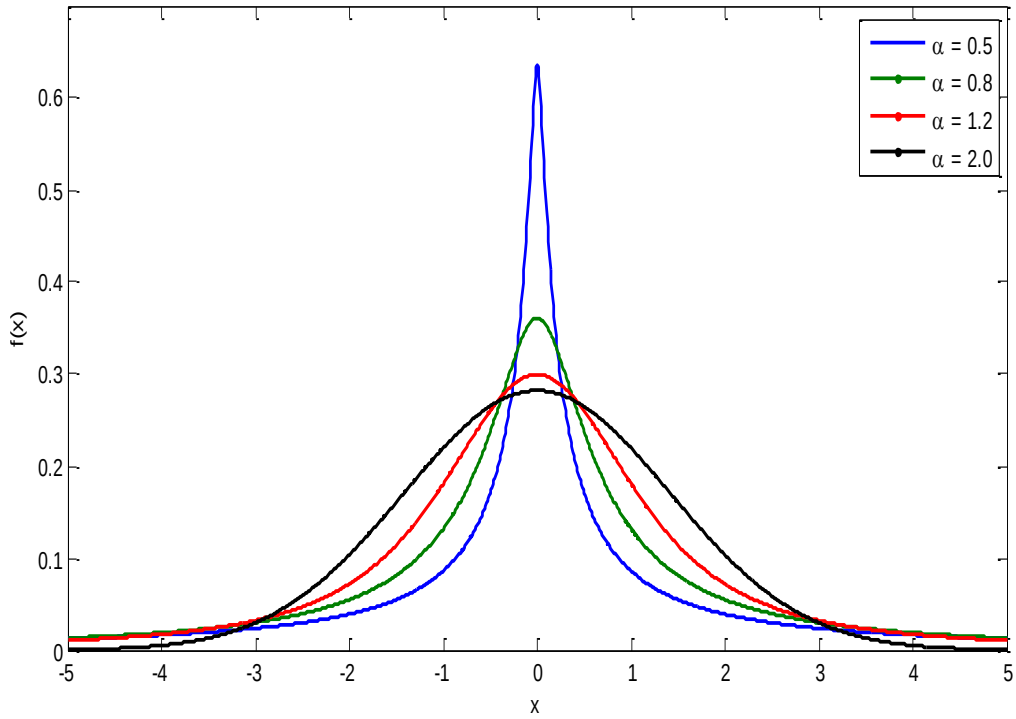

Figure 3.2. Symmetric stable distributions for various α with σ=1.0

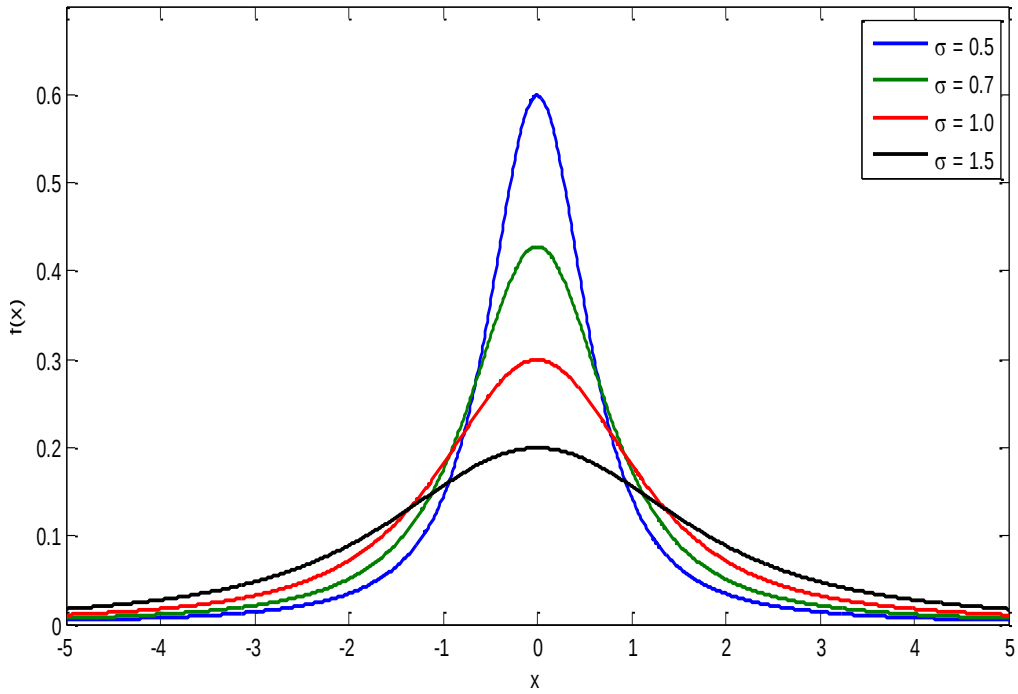

Figure 3.3. Symmetric stable distributions for various σ with α=1.2

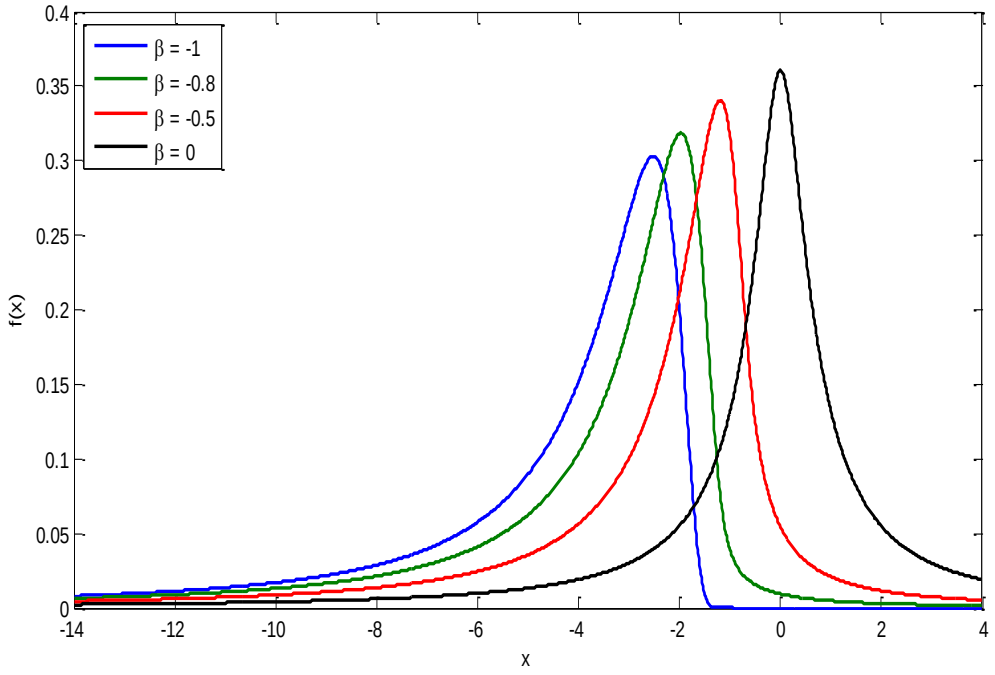

Figure 3.4. Stable distributions for various β with α=0.8 and σ=1.

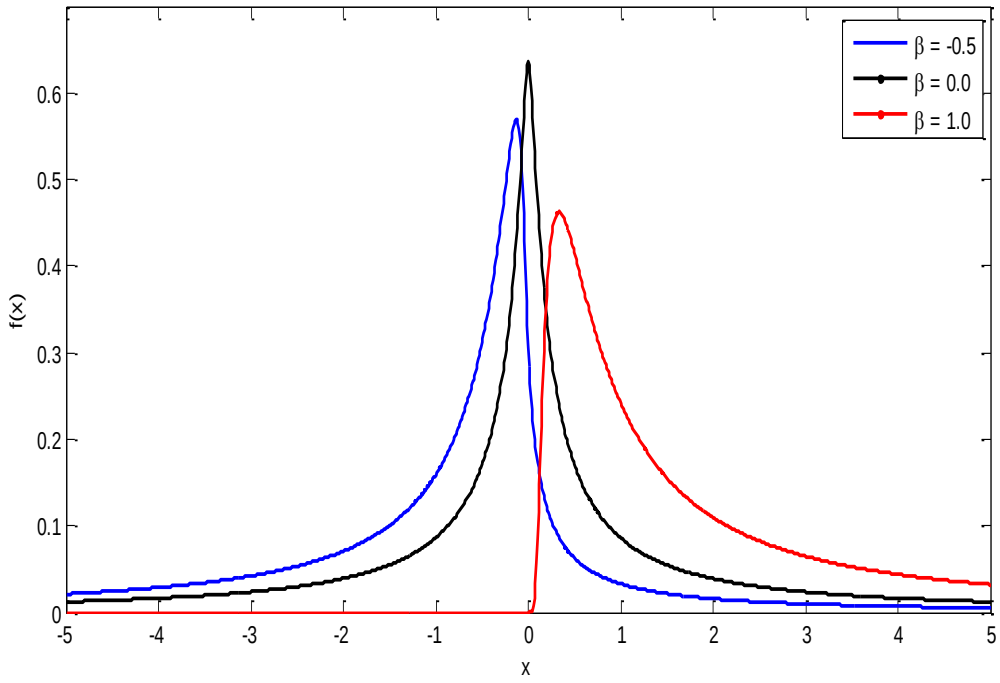

Figure 3.5. Stable distributions for various β with α=0.5 and σ=1.

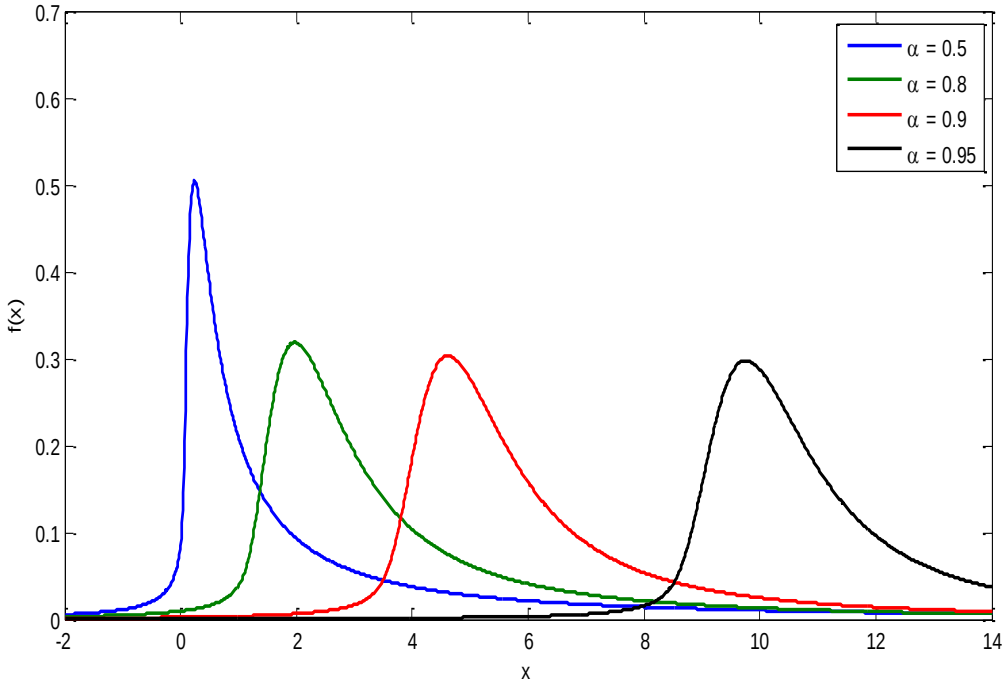

Figure 3.6. Stable distributions for various α with β=0.8 and σ=1.

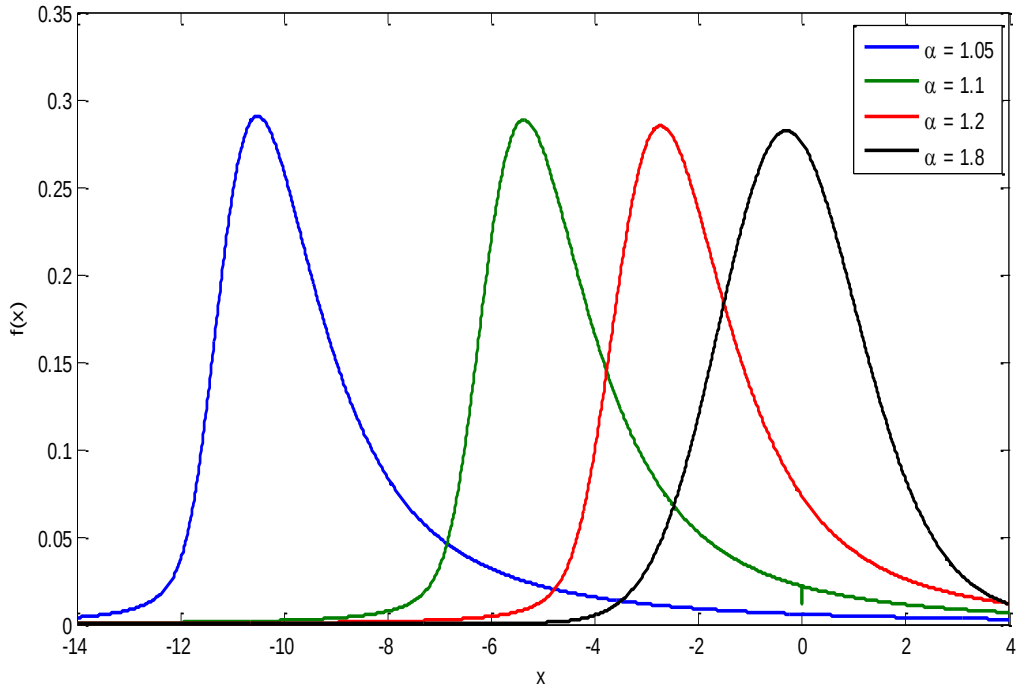

Figure 3.7. Stable distributions for various α with β=-0.8 and σ=1

3.2. Fractional Lower Order Moments (FLOMs)

Moments of a distribution provide important statistical information about the distribution. However integer moments such as second and higher orders are not valid for α-stable distributions. Although the second-order moment of a *SαS* random variable with $0 < \alpha < 2$ does not exist, all moments of order less than α exists and are called the fractional lower order moments (FLOMs) (Shao and Nikias 1993).

The *p*-th order moment for a SαS random variable *X* is defined as

$$E(|X|^p) = C(p,\alpha)\gamma^{\frac{p}{\alpha}}, \quad 1 \le p < \alpha \tag{3.23}$$

where

$$C(p,\alpha) = \frac{2^{p+1}\Gamma\left(\frac{p+1}{2}\right)\Gamma\left(-\frac{p}{\alpha}\right)}{\alpha\sqrt{\pi}\Gamma\left(-\frac{p}{2}\right)} \tag{3.24}$$

and $\Gamma(\cdot)$ is the gamma function defined by

$$\Gamma(\cdot) = \int_0^\infty t^{x-1}\, e^{-t} dt \tag{3.25}$$

Covariation which is analogous to covariance (Shanmugan and Breipohl 1988) can be computed using the fractional lower order moments (FLOM) (Shao and Nikias 1993).

Let *X* and *Y* be jointly *SαS* random variables with $1 < \alpha \le 2$, location parameter $\mu = 0$, and dispersions γ_x and γ_y respectively then the covariation between *X* and *Y* is defined by

$$[X,Y]_\alpha = \frac{E(XY^{<p-1>})}{E(|Y|^p)}\gamma_y \tag{3.26}$$

where

$$z^{<\alpha>} \triangleq \begin{cases} |z|^{\alpha-1}z^*, & \text{z is complex,} \\ |z|^a sign(z), & \text{z is real.} \end{cases} \tag{3.27}$$

It has been also shown that a $S\alpha S$ random variable has also finite negative-order moments (Ma and Nikias 1995).

Let X be a $S\alpha S$ random variable with $\mu = 0$. Then the negative moments are defined as

$$E(|X|^p) = C(p,\alpha)\gamma^{\frac{p}{\alpha}}, \quad -1 < p < \alpha \tag{3.28}$$

where $C(p,\alpha)$ has the same form as in Equation 3.24.

Let X be a $S\alpha S$ random variable with dispersion $\gamma_x > 0$ and the location parameter $\mu = 0$. The norm of X is defined as

$$\|X\|_\alpha = \begin{cases} {\gamma_x}^{1/\alpha} & \text{for } 1 < \alpha \leq 2 \\ \gamma_x & \text{for } 0 < \alpha < 1 \end{cases} \tag{3.29}$$

If $\alpha = 2$ and $E\{X^2\} = \gamma = \frac{\sigma^2}{2}$ then

$$\|X\|_2 = < X, X >^{\frac{1}{2}} = (E\{X^2\})^{\frac{1}{2}} = \frac{\sigma}{\sqrt{2}} \tag{3.30}$$

Thus, the norm $\|X\|_\alpha$ is a scaled version of the dispersion and determines the distribution of X through the characteristic function

$$\varphi(w) = \begin{cases} exp\{-\|X\|_\alpha^\alpha\ |w|^\alpha\}, & 1 \leq \alpha \leq 2 \\ exp\{-\|X\|_\alpha\ |w|^\alpha\}, & 0 < \alpha < 1 \end{cases} \tag{3.31}$$

3.2.1. Fractional Lower-Order Covariance (FLOC)

The covariation does not work when characteristic exponent $\alpha \leq 1$, since it is defined for $1 \leq p < \alpha$.

To overcome this limitation, the fractional-lower order covariance (FLOC) of α-stable distribution is defined as a new measure of similarity (or difference) between two p-th order processes (Ma and Nikias 1996).

The FLOC between the two random process X_1 and X_2 is described as

$$R_{X_1X_2}(\tau) = E[(x_1(t)^{<A>}x_2(t+\tau)^{<B>})] \quad \text{for} \quad 0 \le A < \frac{\alpha}{2}, \qquad 0 \le B < \frac{\alpha}{2} \tag{3.32}$$

where $<\cdot>$ denotes operation as given in Equation 3.27.

The FLOC between two random processes $x_1[n]$ and $x_2[n]$ can be calculated using time average of the sample (Ma and Nikias 1996). If the sample is $\{x_m[1], x_m[2], \cdots, x_m[N]\}$ m=1, 2 then the FLOC is estimated by

$$\hat{R}[k] = \frac{\sum_{n=L_1+1}^{L_2} |x_2[n]|^A \, |x_1[n+k]|^B sign(x_2[n]x_1[n+k])}{L_2 - L_1} \tag{3.33}$$

where $L_1 = \max(0, -k)$, $L_2 = \min(N-k, N)$, $k = [-(N-1), N-1]$

3.3. Parameter Estimation for Skewed-Symmetric Stable Distributions

Several parameter estimators have been proposed in the literature. The methods for parameter estimation with the special case of symmetric stable distributions ($\beta = 0$) have been introduced in (Ma and Nikias 1995). Kuruoglu (2001) has developed estimators for the parameters of skewed α-stable distributions as a generalizations of previously suggested methods for symmetric case.

The characteristic exponent α can be computed by using the sinc estimator (Kuruoglu 2001).

The solution of Equation 3.34 gives the estimate of characteristic exponent α

$$sinc\left(\frac{p\pi}{\alpha}\right) = \left[q\left(\frac{A_pA_{-p}}{tanq} + S_pS_{-p}tanq\right)\right]^{-1} \tag{3.34}$$

where $q = \frac{p\pi}{2}$ and the absolute and signed fractional moments are given as

$$A_p = \frac{1}{n}\sum_{k=1}^{n}|X_k|^p \quad , \quad S_p = \frac{1}{n}\sum_{k=1}^{n} X_k{}^{<p>} \tag{3.35}$$

3.4. Spectral Representations in Impulsive Environments

Suppose that $\{x(n)\}$ is a wide-sense stationary sequence with zero mean. The second-order moment, i.e. the autocorrelation sequence is defined by

$$R_x(k) = E[x(n+k)x(n)] \tag{3.36}$$

where E is the expectation operator and the power spectrum

$$S_x(w) = \sum_{k=-\infty}^{\infty} R_x(k)e^{-jkw} \tag{3.37}$$

Since the α-stable distribution process have no second or higher-order statistics the power spectrum cannot be applied and new spectral analysis are needed to define for impulsive environments.

3.4.1. Covariation Spectrum

In (Jiang and Zha 2008) a fractional order spectrum called covariation spectrum has been proposed.

The covariation spectrum is as the Fourier transform of autocovariation function $R_{XX}(\tau)$:

$$\phi_{xx}(w) = \int_{-\infty}^{\infty} R_{xx}(\tau)\, e^{-jw\tau} d\tau \tag{3.38}$$

where

$$R_{xx}(\tau) \triangleq [x(t), x(t-\tau)]_{\alpha} = \frac{E(x(t)x(t-\tau))^{<p-1>})}{E(|x(t-\tau)|^{p})} \gamma_{x(t-\tau)}, \quad 1 \leq p < a \qquad (3.39)$$

3.4.2. α-Spectrum

Fractional lower-order spectrum named α-spectrum of the output is defined in (Ma and Nikias 1995) as:

$$S_{\alpha}(z) = [Y_n, W_n(z)]_{\alpha} = \left[Y_n, \sum_{i=-q}^{i=q} Y_{n-i} z^{i} \right]_{\alpha} = \gamma_x H \left(\left(\frac{1}{z} \right)^{<\alpha-1>} \right) (H(z))^{<\alpha-1>} \qquad (3.40)$$

where $[Y_n, W_n]_{\alpha}$ is the generalized output covariation ,$W_n(z)$ is the windowed z-transform of the channel output Y_n

$$W_n(z) = \sum_{i=-q}^{q} Y_{n-i} z^{i} \qquad (3.41)$$

and the input-output relation of the linear system with impulse response h_k is given by the convolution sum

$$Y_n = \sum_{k=0}^{q} h_k X_{n-k} \qquad (3.42)$$

and the z-transform of the impulse response is as

$$H(z) = \sum_{n=0}^{q} h_n z^{-n} \qquad (3.43)$$

h_k is impulse response coefficients of finite impulse response system and the input X_n is i.i.d *SαS* random variable with dispersion γ_X.

The α-spectrum of the output $S_{\alpha}(z)$ calculated on the unit circle $|z| = 1$ is

$$S_\alpha(e^{jw}) = \gamma_X H(e^{jw})(H(e^{jw}))^{<\alpha-1>} = \gamma_X |H(e^{jw})|^\alpha \tag{3.44}$$

This relation coincides with the relation in (Shanmugan and Breipohl 1988) for $\alpha = 2$.

In (Jiang and Zha 2008) the connection between α-spectrum and covariation spectrum has been proved such that α-spectrum on unit circle is q-order interceptive form of covariation spectrum

$$\phi_{xx}(w) = \lim_{q\to\infty} \{S_\alpha(z)\}^*|_{z=e^{jw}} \tag{3.45}$$

3.4.3. Fractional Lower order Pseudo Power Spectrum (FLOPPS)

A fractional lower order pseudo power spectrum (FLOPPS) or in short pseudo-power spectrum (PPS) has been defined to analyze better frequency domain characteristics of alpha-stable distribution noise in (Jiang, Huang et al. 2010).

The α-stable distribution signal has no second-order moments hence no power spectrum. However sampled sequences *x(n)* can be transformed to $\tilde{x}(n)$

$$\tilde{x}(n) \triangleq x(n)^{<p/2>}, \quad 0 \le p < \alpha \tag{3.46}$$

where $<\cdot>$ is defined as in Equation 3.27.

Then the autocorrelation function of $\tilde{x}(n)$ is

$$\begin{aligned} r(l) &= E[\tilde{x}(n)\tilde{x}^*(n-l)] = E\left[x(n)^{<\frac{p}{2}>} x^*(n-l)^{<\frac{p}{2}>}\right] \\ &= E[|x(n)|^p]\delta(l) = C(p,\alpha)\gamma^{\frac{p}{\alpha}}\delta(l), \qquad 0 < p < \alpha < 2 \end{aligned} \tag{3.47}$$

The FLOPPS is calculated as the Fourier transform of the autocorrelation function of transformed signal

$$R(e^{jw}) = \sum_{l=-\infty}^{\infty} r(l)e^{-jwl} = C(p,\alpha)\gamma^{\frac{p}{\alpha}} \tag{3.48}$$

All processes are assumed to be stationary in the estimation of α-spectrum and covariation spectrum. Since these spectrums are not applicable to non-stationary signals, we need to define a new approach for the spectrum analysis of non-stationary processes in an impulsive environment. The next section presents the time-varying spectral representation.

3.5. Time-Frequency Analysis

Time-frequency representation (TFR) are useful tools for analyzing the behavior of non-stationary signals whose spectral properties change with time.

The Wigner Ville distribution (WVD) is one of the quadratic time frequency representations (QTFR). The WVD can be used to analyze signals that are contaminated by noise that is Gaussian. The chaotic waveforms have also been analyzed in the time-frequency domain especially by Wigner distribution because of the non-stationary nature of the chaotic waveforms (Özkurt 2004). However in the presence of additive impulsive noise the WVD can be severely degraded and any information about the desired signal is lost. A robust Wigner Ville distribution using fractional lower order statics (FLOS), called as fractional lower order Wigner Ville Distribution (FLOWVD), which is capable of analyzing non-stationary signals in impulsive environment has been introduced in (Griffith Jr, Gonzalez et al. 1997). This method combines the traditional WVD with the FLOC. On the other hand, a robust FLOS-based Polynomial Wigner Ville Distribution, Fractional Lower-Order Polynomial Wigner-Ville Distribution (FLOPWVD) has been introduced in (Djeddi and Benidir 2004).

3.5.1. Wigner-Ville Distribution

Wigner Ville spectrum is an effective tool of time-frequency analysis for non-stationary random processes. The Wigner distribution of the signal $x(t)$ is expressed as

$$W_x(t,f) = \int_{-\infty}^{\infty} x\left(t+\frac{\tau}{2}\right) x^*\left(t-\frac{\tau}{2}\right) e^{-j2\pi f\tau} d\tau \tag{3.49}$$

For the given associated spectrum $X(w)$ of the signal $x(t)$, WVD has the following form in the frequency domain

$$W_X(t,f) = \int_{-\infty}^{\infty} X\left(f+\frac{\theta}{2}\right) X^*\left(f-\frac{\theta}{2}\right) e^{-j2\pi f\theta} d\theta \tag{3.50}$$

A discrete-time WVD (DWVD) has the form

$$W_x(t,f) = 2\sum_{m} x(n+m)x^*(n-m)e^{-j4\pi nf/f_s} \tag{3.51}$$

where f_s is the sampling rate.

The most critical properties of WVD are listed as:

Property 3.5.1.1 WVD conserves total energy

$$E_x = \int_{-\infty}^{\infty}\int_{-\infty}^{\infty} W_x(t,f)dfdt \tag{3.52}$$

Property 3.5.1.2 WVD satisfies marginal properties

$$\int_f W_x(t,f)df = |x(t)|^2 \tag{3.53}$$

$$\int_t W_x(t,f)df = |X(f)|^2 \tag{3.54}$$

Property 3.5.1.3 If a signal *y* is the convolution of *x* and *h*, the WVD of *y* is the convolution in time between the WVD of *x* and the WVD of *h*

$$y(t) = \int_{-\infty}^{\infty} h(t-u)x(u)du \tag{3.55}$$

$$\Rightarrow W_y(t,f) = \int_{-\infty}^{\infty} W_h(t-u,f) W_x(u,f) du$$

3.5.2. The Evolutive Spectrum

Since the WVD is formed by taking the Fourier transform of the autocorrelation of a signal $x(t)$ with respect to the delay variable τ, the evolutive spectrum of a random process is defined as (Griffith Jr, Gonzalez et al. 1997)

$$S_x(t,f) = \int_{\tau} E\left\{x\left(t+\frac{\tau}{2}\right) x^*\left(t-\frac{\tau}{2}\right)\right\} e^{-j2\pi f\tau} d\tau \tag{3.56}$$

By interchanging the integration and expectation operators, the evolutive spectrum can be interpreted as the expectation of all the WVDs corresponding to their respective members of the ensemble of random processes $\{x(t)\}$,

$$S_x(t,f) = E\{W_x(t,f)\} \tag{3.57}$$

The evolutive spectrum for discrete time stochastic signals is described as

$$S_x(n,F) = \sum_{m} R_x(n,m) e^{-j2\pi mF} \tag{3.58}$$

where $R_x(n,m) = E\{x(n+m)x^*(n-m)\}$ is the autocorrelation function of the stochastic process $\{x(n)\}$.

3.5.3. Fractional Lower Order Wigner Ville Distribution (FLOWVD)

In the presence of α-stable noise, second-order measures such as the autocorrelation function and the higher-order moments of signals become unbounded and variance could not use as a measure of dispersion. Since the evolutive spectrum is based on the use of the autocorrelation function for calculating the power spectrum, it

becomes useless for characterizing impulsive noise processes such as α-stable signals ($\alpha < 2$).

The solution to this problem has been introduced in (Griffith Jr, Gonzalez et al. 1997) by defining a new WVD based on fractional-lower order covariance measure.

The Fourier transform of the FLOC defined as in (3.44) is as fractional lower-order evolutive spectrum

$$S_x{}^{<\alpha>}(t,f) = \mathcal{F}\{FLOC\}$$
$$S_x{}^{<a>}(t,f) = \int_\tau E\{x^{<a>}(t+\tau/2)x^{<-a>}(t-\tau/2)\}e^{-j2\pi f\tau}d\tau \tag{3.59}$$

which is the expectation of an ensemble of TFRs of the form (FLOWVD)

$$W_x{}^{<a>}(t,f) = \int_\tau x^{<a>}(t+\tau/2)x^{<-a>}(t-\tau/2)e^{-j2\pi f\tau}d\tau \tag{3.60}$$

i.e, $S_x{}^{<\alpha>}(t,f) = E\{W_x{}^{\alpha}(t,f)\}$ is similar to Equation 3.57.

The discrete-time version of fractional lower-order Wigner Ville distribution (FLOWVD) is in the form

$$W_x{}^{<\alpha>}(n,f) = 2\sum_m x^{<\alpha>}(n+m)x^{-<\alpha>}(n-m)e^{-j4nmf} \tag{3.61}$$

The FLOWVD is itself a standard WVD, where the input signal is $x^{<a>}(n)$ rather than $x(n)$ and has the following properties (Griffith Jr, Gonzalez et al. 1997):

Property 3.5.3.1 The FLOWVD is real i.e.,

$$W_x{}^{<p>}(n,f) = \left[W_x{}^{<p>}(n,f)\right]^* . \tag{3.62}$$

Property 3.5.3.2 The FLOWVD is time-invariant for all p where $0 < p < \alpha$.

If $x(n) = r(n-n_0)$ then

$$W_x^{<p>}(n,f) = W_r^{<p>}(n-n_0,f). \tag{3.63}$$

Property 3.5.3.3 The FLOWVD is frequency-invariant.

If $x(n) = r(n)e^{j2\pi f_0 n}$, where $f_0 < f_a - f_{max}$ and f_{max} is the supremum of the support of X(f) in the interval $[-f_a, f_a]$, then

$$W_x^{<p>}(n,f) = W_r^{<p>}(n,f-f_0). \tag{3.64}$$

Property 3.5.3.4 The marginal energy density with respect to time is

$$\int_f W_x^{<p>}(n,f)df = |x(n)|^{2p}\,. \tag{3.65}$$

CHAPTER 4

CHUA'S CIRCUIT

4.1. Introduction

Most real-world phenomena are nonlinear and linear systems are not able to describe the real world but only are valid for certain ranges of physical variables. Rich repertoire of nonlinear dynamic systems may display a variety of behaviors such as limit-cycle, bifurcation and chaos.

Chaos can be defined as aperiodic long-term behavior in a deterministic system that exhibits sensitive dependence on initial conditions (Strogatz). Aperiodic long-term behavior means that the system's trajectories do not settle down to fixed points or periodic orbits as time tends to infinity.

The most important property of chaotic systems is sensitive dependence on initial conditions. This property implies that a slightest change in the initial conditions can cause a completely different behavior in the output. The other properties are given as (Parker and Chua 1987).

i) Trajectories are bounded,

ii) the limit set for a chaotic behavior is related to fractals and Cantor sets,

iii) chaotic systems have noise-like spectrum.

Chaos theory has been applied in many scientific and engineering disciplines such as mathematics, physics, chemistry, economics, biology, ecology, mechanical systems, nonlinear electronic circuits and secure communication (Pecora and Carroll 1990) (Cuomo and Oppenheim 1993) in which two synchronized sequences of chaotic signals can be used for encoding private electronic communications. It has been also shown that the sensitivity of chaotic systems to small perturbations can be used to stabilize or control the systems. Since a chaotic system is composed of an infinite number of unstable periodic orbits, the trajectories can be directed to a desired periodic

orbit. This is done by perturbing the input parameters just enough to make the system on that closed orbit when the trajectory comes nearby the desired periodic orbit.

Similar efforts are being made to control epileptic brain seizures which exhibit chaotic behavior (Schiff, Jerger et al. 1994).

Chua's circuit is an example of a chaotic system. It can be easily implemented in many different ways. An experimental confirmation of n-double scrolls has been given by (Gotz, Feldmann et al. 1993). Higher dimensional Chua's circuits have been investigated in (Chua, Wu et al. 1993). Secure communications via chaotic synchronization have been experimentally demonstrated using Chua's circuit (Parlitz, Chua et al. 1992; Cuomo and Oppenheim 1993).

In the rest of the chapter the Chua circuit is investigated in detail.

4.2. Chua's Circuit

Chua's circuit is the simplest autonomous circuit which exhibits a rich variety of dynamical behaviors including bifurcations and chaos. It can be constructed by three linear elements (one inductor and two capacitors) and one nonlinear resistor experimentally. The behavior of the Chua's circuit with respect to its parameters has been extensively studied both in simulations and experiments in many papers (Parker and Chua 1987; Chua, Wu et al. 1993).

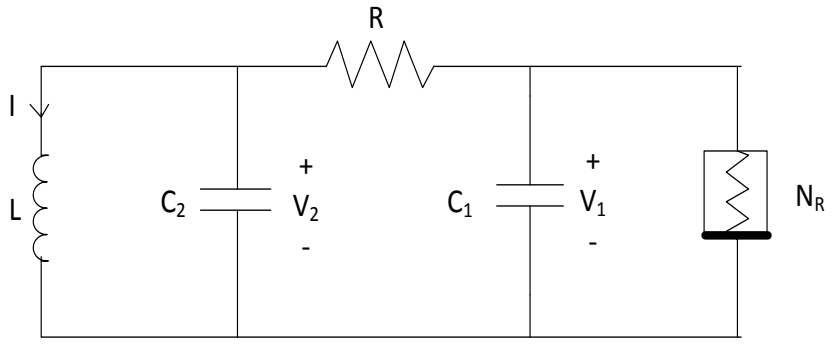

Figure 4.1. Chua's Circuit

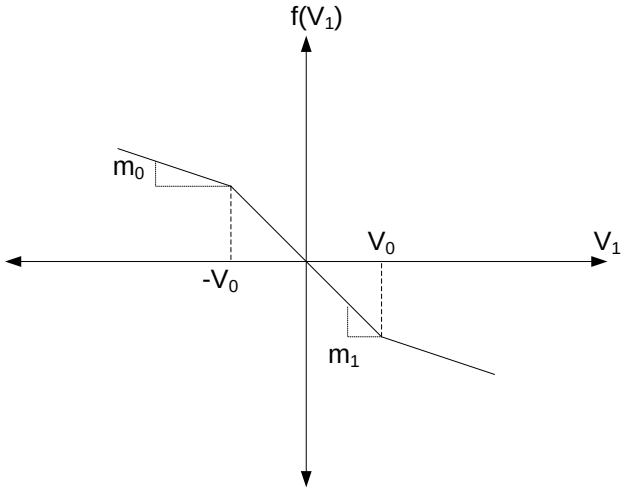

Figure 4.2. Chua's Circuit nonlinear characteristic function

The dynamics of autonomous Chua circuit is described by the following set of three differential equations (Parker and Chua 1987)

$$\begin{aligned} L\frac{dI}{dt} &= -V_2 \\ C_1\frac{dV_1}{dt} &= \frac{(V_2 - V_1)}{R} - f(V_1) \\ C_2\frac{dI}{dt} &= -\frac{(V_1 - V_2)}{R} + I \end{aligned} \tag{4.1}$$

where V_1 and V_2 are the voltages across capacitors C_1 and C_2 respectively, I is the current through the inductor and the characteristic of nonlinear resistor N_R described by the piecewise-linear function $f(V_1)$ is given as

$$f(V_1) = m_1 V_1 + \frac{m_0 - m_1}{2}(|V_1 + V_0| - |V_1 - V_0|) \tag{4.2}$$

By making the following changes

$$x = \frac{V_1}{V_0}, y = \frac{V_2}{V_0}, \quad z = \frac{IR}{V_0},$$
$$\alpha = \frac{C_2}{C_1}, \ \beta = \frac{C_2 R^2}{L}, \tag{4.3}$$
$$\widetilde{m_0} = \frac{m_0}{V_0}, \quad \widetilde{m_1} = \frac{m_1}{V_0}, \quad \tau = \frac{t}{RC_2}$$

The dimensionless form of Equation 4.1 is obtained as

$$\begin{aligned} \dot{x} &= \alpha(x - y - f(x)) \\ \dot{y} &= x - y + z \\ \dot{z} &= -\beta y \end{aligned} \tag{4.4}$$

where

$$f(x) = \widetilde{m_1} x + \frac{\widetilde{m_0} - \widetilde{m_1}}{2}(|x+1| - |x-1|) \tag{4.5}$$

4.2.1. The Chua's Circuit Driven by α-Stable Noise

The equations describing the nonautonomous Chua's circuit driven by α-stable noise shown in Figure 4.3 are defined by

$$\begin{aligned} L\frac{dI}{dt} &= -V_2 + E(t) + \xi(t) \\ C_1\frac{dV_1}{dt} &= \frac{(V_2 - V_1)}{R} - f(V_1) \\ C_2\frac{dI}{dt} &= -\frac{(V_1 - V_2)}{R} + I \end{aligned} \tag{4.6}$$

where $E(t) = E_0 \sin(2\pi f_0 t)$ represents the external deterministic forcing signal and $\xi(t)$ indicates α-stable noise and the piecewise nonlinear function is as Equation 4.5.

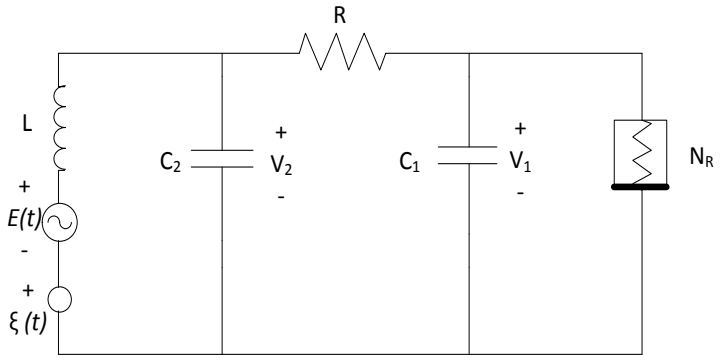

Figure 4.3. Chua's circuit driven by α-stable noise

In our study the parameters of dimensionless form of autonomous Chua' circuit are selected to be such that

$$\alpha = 8.5,\ \ \beta = 100/7,\ \ \widetilde{m_1} = -8/7,\quad \widetilde{m_0} = -5/7 \tag{4.7}$$

4.3. Harmonic Balance Method

The aim of this section is to provide the approximation behavior of nonlinear dynamic system for the given parameters and compute the oscillation frequency theoretically which will be compared with the one obtained from simulation results.

The chaotic behavior of nonlinear dynamic system is investigated by the harmonic balance method (Genesio and Tesi 1991; Genesio and Tesi 1992). The method focuses on determination and stability analysis of equilibrium points and limit cycles of nonlinear dynamic systems.

The dynamic system is governed by the form

$$q(D)y(t) + p(D)f(y) = 0 \tag{4.8}$$

where y(t) denotes the output of system, D is the differential operator, $p(\cdot)$ and $q(\cdot)$ are two polynomial operators and $f(\cdot)$ is a nonlinear real valued function.

The system described by Equation 4.8 can be considered as a feedback structure shown as in Figure 4.4 where the linear part can be modeled by the transfer function $L(s) = \frac{p(s)}{q(s)}$ and the nonlinear subsystem is represented by the single-valued real function *N(y).*

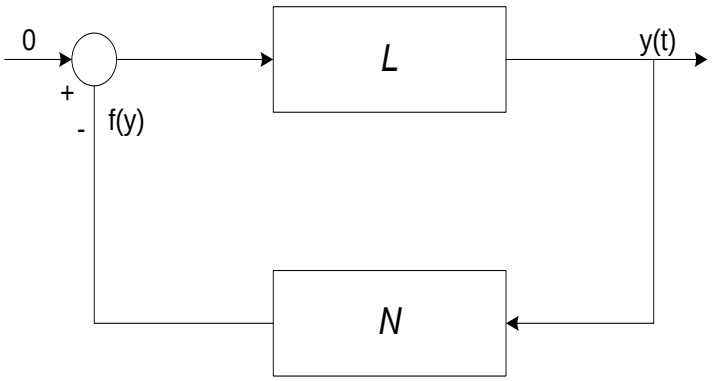

Figure 4.4. Lur'e form

Conjecture (Genesio and Tesi 1989): A Lur'e feedback system presents chaotic behavior when a stable predicted limit cycle (PLC) and an unstable equilibrium point (EP) interact with a suitable filtering effect along the system.

The conjecture can be reduced to the satisfying the following conditions:

i) existence of a seperate unstable EP,

ii) existence of a stable LC,

iii) interaction between LC and EP,

iv) suitable filtering effect along the system.

4.3.1. Existence of an Equilibrium Point

The equilibrium points are the solution of Equation 4.8 which satisfy

$$y_e + L(0)f(y_e) = 0 \tag{4.9}$$

Apart from the singularity occurring at $y_e = 0$, the other equilibrium point must satisy the relation

$$\frac{f(y_e)}{y_e} + \frac{1}{L(0)} = 0 \tag{4.10}$$

The stability of equilibrium points can be checked by linearizing $f(y)$ at y_e and by determining the eigenvalues of the linearized system.

4.3.2. Existence of a Predicted Limit Cycle (PLC)

It is known that there must exist at least two limit cycles for the chaotic motion. Therefore the conditions for the presence of limit cycle can be done approximately by the well-known describing function method.

The solution of the Equation 4.8 is assumed in the form

$$y(t) = a_0 + a_1 \sin(wt), \quad a_1, w > 0 \tag{4.11}$$

The corresponding output f(y) is expanded in Fourier series as

$$f\big(y(t)\big) = N_0(a_0, a_1)a_0 + N_1(a_0, a_1)a_1 \sin(wt) + \cdots \tag{4.12}$$

The nonlinear system N is characterized by the dual describing function terms as:

$$N_0(a_0, a_1) = \frac{1}{2\pi a_0}\int_{-\pi}^{\pi} f(a_0 + a_1 \sin\phi)d\phi \tag{4.13}$$

$$N_1(a_0, a_1) = \frac{1}{\pi a_1}\int_{-\pi}^{\pi} f(a_0 + a_1 \sin\phi)\sin\phi d\phi \tag{4.14}$$

By discarding the higher harmonics in Equation 4.12 and substitute the Equations 4.11, 4.13 and 4.14 into the dynamic system governed by 4.8 then the conditions given below are obtained

$$L(0)N_0(k_0, k_1) = -1$$
$$L(jw)N_1(k_0, k_1) = -1 \tag{4.15}$$

A PLC must satisfy the conditions given in Equation 4.15.

4.3.3. Interaction of PLC and EP

The condition expressing the possibility of interaction between the PLC and EP follows from the solutions of equations 4.11 and 4.15 in the form

$$|y_e - a_0| \leq a_1 \tag{4.16}$$

4.3.4. Filtering effect

The accuracy of the prediction of limit cycles for the system (4.8) is based on the filtering effect which was approximately translated in

$$|L(jw)| \gg |L(jkw)|, \quad k = 2,3,\cdots \tag{4.17}$$

The condition requires a suitable filtering effect of the system in the sense that high values of this element ensure a pure oscillation corresponding to the PLC, whereas its reduction leads to a domain of parameters where the chaotic behaviour occurs.

Hence the final behaviour of the system under consideration depends on its filtering properties.

4.4. Chaos Prediction on Chua's Circuit Using Harmonic Balance Method

Chua circuit can be transformed into the following third-order scalar differential equation

$$\frac{\partial^3 x}{\partial \tau^3} + (1+\alpha)\frac{\partial^2 x}{\partial \tau^2} + \beta\frac{\partial x}{\partial \tau} + \beta\alpha x + \alpha\left(\frac{\partial^2 f(x)}{\partial \tau^2} + \frac{\partial f(x)}{\partial \tau} + \beta f(x)\right) = 0 \qquad (4.18)$$

From a system theoretical point of view Chua's circuit can be considered as a particular case of a Lur'e system.

The corresponding linear part is described by

$$L(s) = \frac{p(s)}{q(s)} = \frac{\alpha(s^2 + s + \beta)}{s^3 + (1+\alpha)s^2 + \beta s + \alpha\beta} \qquad (4.19)$$

For the nonlinear part the piecewise linear function given in Equation 4.5 is replaced with a smooth cubic function given as

$$f(x) = k_0 x + k_1 x^3 \qquad (4.20)$$

This is done by a least square fit of the cubic function to the piecewise-linear function over an interval approximation $[-d, d]$ (Gonzalo 2010) where

$$k_0 = \frac{\widetilde{m_1} + (45d^4 - 50d^2 + 21)(\widetilde{m_0} - \widetilde{m_1})}{16d^5}, \qquad (4.21)$$

and

$$k_1 = \frac{-35(d_2 - 1)^2(\widetilde{m_0} - \widetilde{m_1})}{16d^7}. \qquad (4.22)$$

For the parameters $\widetilde{m_1} = -8/7$, $\widetilde{m_0} = -5/7$ and $d = 2$ corresponding smooth cubic parameters are obtained as $k_0 = -1.1671$ and $k_1 = 0.0659$.

Since this cubic function preserves the dynamical behavior of original piecewise function, we use the cubic function to represent the characteristics of nonlinear resistor so that it provides computational facility in our theoretical analysis.

$L(0) = 1$ is found from Equation 4.15 and since $f(x) = k_0 x + k_1 x^3$ and the equilibrium points which are solutions of Equation 4.9 are calculated as

$$x_{e_1}^+ = -1.5923, \qquad x_{e_0} = 0, \quad x_{e_1}^- = 1.5923 \qquad (4.23)$$

Equations 4.13-4.14 can be solved with respect to a_0, a_1 and w to give the parameters of approximate periodic solutions in the form of Equation 4.11.

Since $N_1(k_0, k_1)$ is a real number then from Equation 4.15

$$Im\big(L(jw)\big) = 0 \tag{4.24}$$

is obtained.

Hence the oscillation frequency *w* of the PLC can be found using Equation 4.24 and it depends only on the linear part of the system.

Substituting Equation 4.20 into Equation 4.24 and solving for w,

$$w^2 = \beta - \left(\frac{1+\alpha}{2}\right) \mp \left[\left(\frac{1+\alpha}{2}\right)^2 - \beta\right]^2 \tag{4.25}$$

gives two real values for the characteristic frequency $w_1 = 2.5805$ and $w_2 = 3.5232$.

Substituting Equation 4.9 into Equation 4.13 and 4.14 the describing function terms are obtained as

$$N_0(a_0, a_1) = k_0 + k_1 {a_0}^2 + \frac{3}{2} k_1 {a_1}^2 \tag{4.26}$$

$$N_1(a_0, a_1) = k_0 + 3k_1 {a_0}^2 + \frac{3}{4} k_1 {a_1}^2 . \tag{4.27}$$

The application of harmonic balance with Equation 4.15 yields the parameters

$$\widehat{a_0} = \mp \sqrt{\frac{1-k_0}{5k_1} - \frac{2}{5k_1 L(jw)}}, \qquad \widehat{a_1} = \sqrt{\frac{-12-8k_0}{15k_1} + \frac{4}{15k_1 L(jw)}} \tag{4.28}$$

Equation 4.28 requires the following predicted limit cycle (PLC) condition

$$L(jw) < \frac{1}{3 + 2k_0}. \tag{4.29}$$

For $L(jw_1) = 1.1145$, parameters are evaluated such as

$$\widehat{a_0} = \mp 1.0634 \text{ and } \widehat{a_1} = 0.9678. \tag{4.30}$$

The stability of the PLCs can be checked by the application of the Loeb criterion (Tesi, Abed et al. 1996)

$$\left.\frac{\partial N_1(a_0(a_1), a_1)}{a_1}\right|_{a_1} . Im\left\{\frac{\partial}{\partial w} L(jw)|_w\right\} < 0 \tag{4.31}$$

Since *L(jw)* is real-valued, the Loeb stability condition reduces to the condition

$$\left.\frac{\partial N_1(a_0(a_1), a_1)}{a_1}\right|_{a_1} < 0. \tag{4.32}$$

The condition of interaction given in Equation 4.16 is also satisfied that there is no interaction between the PLCs and equilibrium points

$$|x_e - \widehat{a_0}| \leq \widehat{a_1} \tag{4.33}$$

For the autonomous Chua's circuit parameters given as below

$$\alpha = 8.5, \ \beta = 100/7, \qquad \widetilde{m_1} = -8/7, \quad \widetilde{m_0} = -5/7 \tag{4.34}$$

the largest Lyapunov exponent has been also computed as 0.3167 which is positive as expected (Strogatz ; Parker and Chua 1987).

According to harmonic balance method two symmetrical predicted limit cycles with respect to the origin have been observed for the chosen parameters and they have projections on x around the equilibrium points.

CHAPTER 5

SIMULATION RESULTS

In this chapter the simulation results provide the main results of this research. The circuit proposed in Chapter 4 is simulated by means of a Runge Kutta integration rule with step size $h = 0.05$.

In the absence of an external noise a phase trajectory belongs to either one or another attractor depending on the initial conditions shown as in Figure 5.1. The parameters of Chua circuit have been chosen in such a way that two single-scroll symmetrical attractors are present in the absence of external forcing and which attractor is chosen depends on initial conditions.

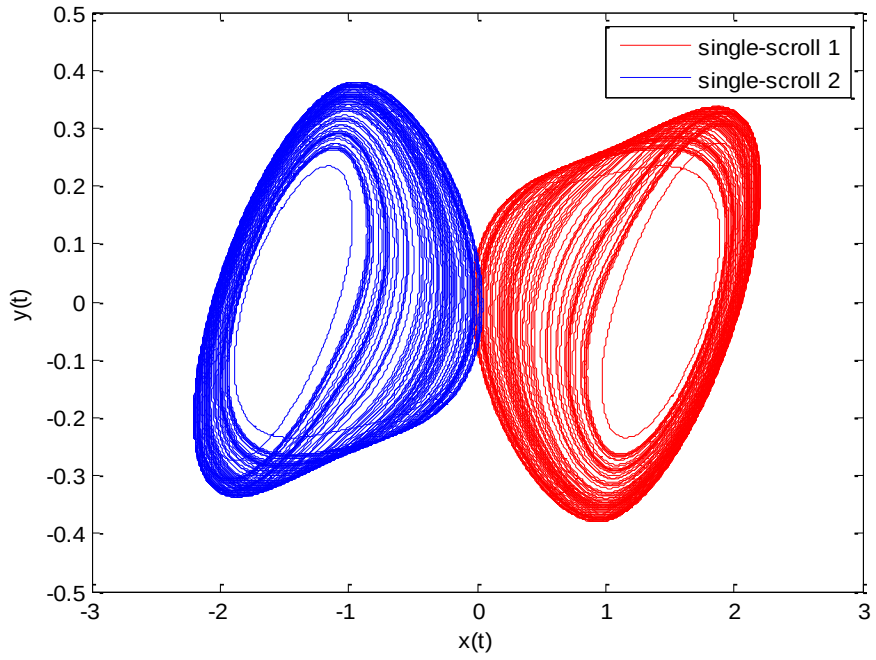

Figure 5.1. Two symmetrical single-scroll attractor

The voltage $x(t)$ and its power spectrum are shown in Figure 5.2 and Figure 5.3, respectively.

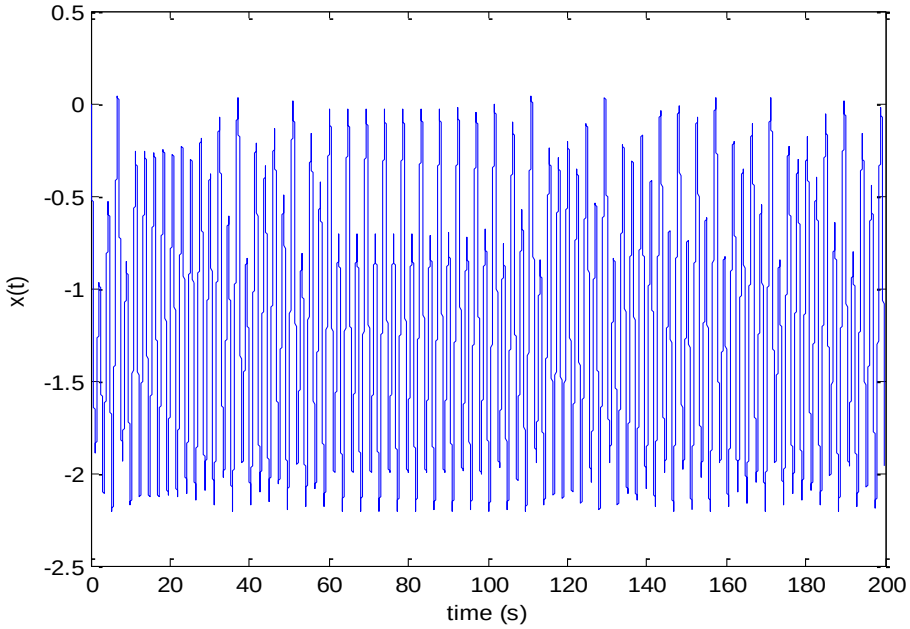

Figure 5.2. Voltage on *x(t)* for one single-scroll attractor

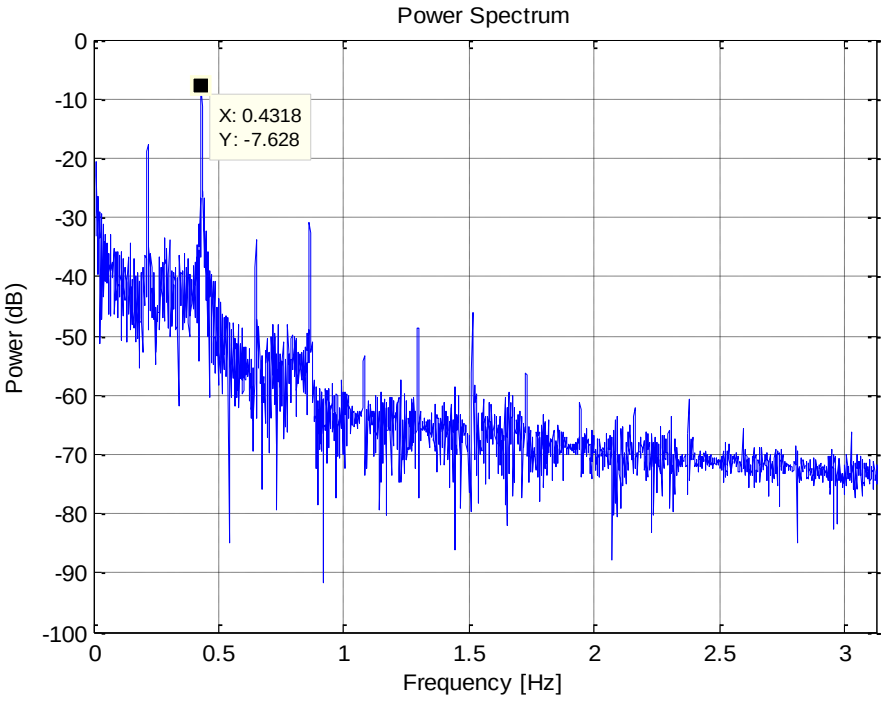

Figure 5.3. Power Spectrum of Autonomous Chua Circuit

The power spectrum confirms the chaotic nature since it has continuous broadband spectrum. The characteristic (oscillation) frequency of autonomous Chua's circuit is indicated as a maximum in the power spectrum and denoted as f_{ch}. The maximum peak is located at $f_{ch} = 0.4318$ Hz ($w_{ch} = 2.7131$ rad/s). It coincides with the analytical result which is found approximately $w_{ch} = 2.5805$ rad/s in Chapter 4. The spectrum is also characterized with several peaks at other relatively high frequencies.

Without noise and external forcing there is no possibility to jump from one attractor to the other. However the presence of external periodic forcing signal can induce jumps between the attractors only if it is suprathreshold which means its amplitude is above a certain threshold value. A minimum amplitude value of periodic signal required to induce jumps is determined as a function of its frequency. This threshold value is plotted as a function of the ratio of input frequency f_0 to the characteristic frequency f_{ch} in Figure 5.4.

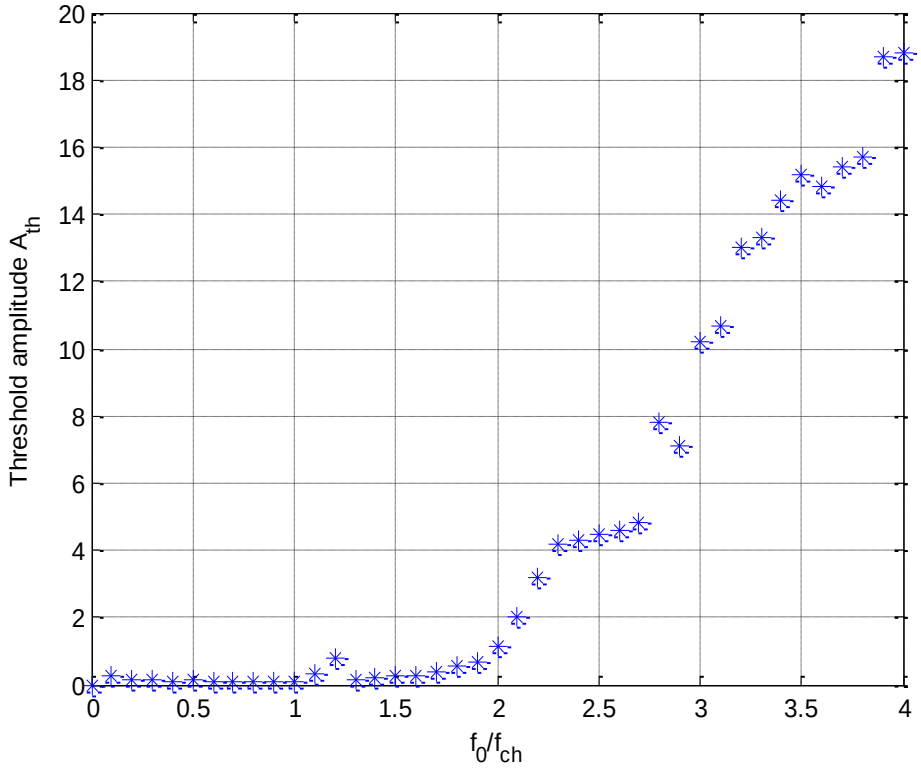

Figure 5.4. The dependence of the threshold value of the external periodic forcing signal on its frequency f_0.

The results indicate that the threshold amplitude is relatively low for low frequencies. At high frequencies the threshold amplitude to induce jumps increases. If we look into the Figure 5.4 and then it is realized that the threshold is low when it is close to the characteristic frequency and it increases for smaller and larger frequencies.

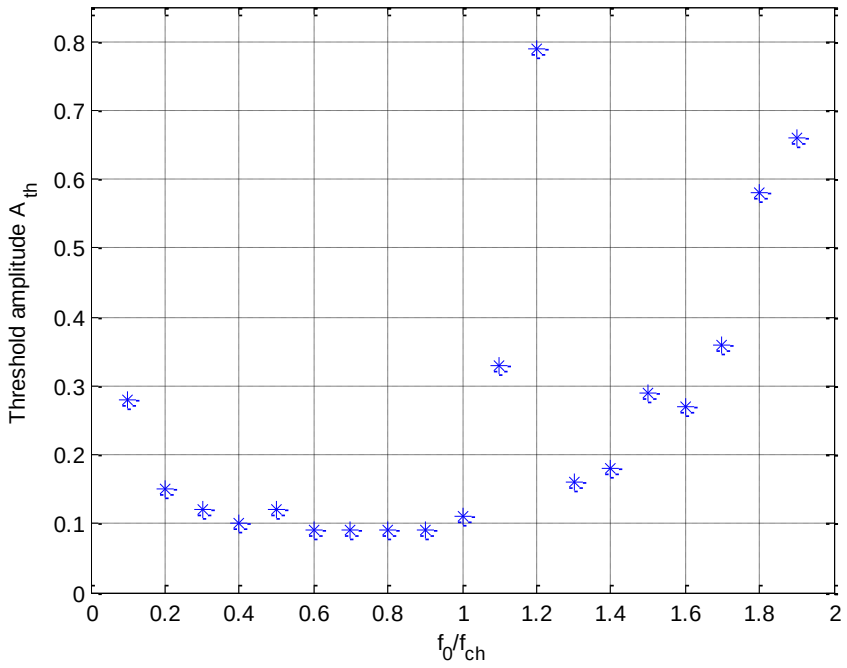

Figure 5.5. Threshold value of the external periodic signal as a function of the ratio of its frequency f_0 to the characteristic frequency f_{ch}.

The frequency of the external periodic forcing is set at $f_0 = 0.34544\ Hz$ where $f_0/f_{ch} = 0.8$ corresponds to the region around the lowest value of threshold amplitude. Since we want to induce jumps between the attractors by the addition of noise, the amplitude of the external forcing is set close to but below the minimum threshold value to ensure that the input signal is sub-threshold. Under these conditions, the addition of small amount of noise enables to induce jumps between the attractors.

In this section, spectral power amplification (SPA) denoted by η, has been used to quantify the stochastic resonance. Since we deal with the non-stationary signals, we need to describe the power in terms of time and frequency. Therefore, we use fractional lower order Wigner Ville distribution (FLOWVD) which is the modification of WVD in impulsive environments described in Chapter 3.

In order to characterize the noise-dependent amplification, we define a spectral amplification parameter

$$\eta = \frac{S_{out}(w_i)}{S_{out}(w_i)|_{\sigma=0}} \tag{5.1}$$

where w_i is the frequency (rad/s), $S_{out}(w_i)$ is the power spectral density of output at the input frequency, $S_{out}(w_i)|_{\sigma=0}$ is the power spectral density of output at the input frequency in the absence of noise signal and σ is a scale parameter of external α-stable noise.

The amplification of the sub-threshold input periodic signal as a function of the noise intensity with $\beta = 0$ is shown as in Figures 5.6-5.10 whereas with $\beta = 1$ is shown as in Figures 5.11-5.12 and with $\beta = -1$ in Figures 5.13-5.14. The results have been averaged over 50 realizations.

All simulations show a visible stochastic resonance (SR) effect in Chua's circuit driven by α-stable noise with $\beta = 0$, $\beta = 1$ and $\beta = -1$. Figures also show multiple maxima as a function of noise scale parameter which is called stochastic multi-resonance (SMR) (Vilar and Rubi 1997). The SR effect fades as the noise grows more impulsive (Kosko and Mitaim 2001) (Kosko and Mitaim 2003). The optimal scale parameter σ_{opt} becomes smaller as the noise becomes more impulsive. σ_{opt} is the value of noise scale parameter in which the SPA has a maximum and the SR effect occurs.

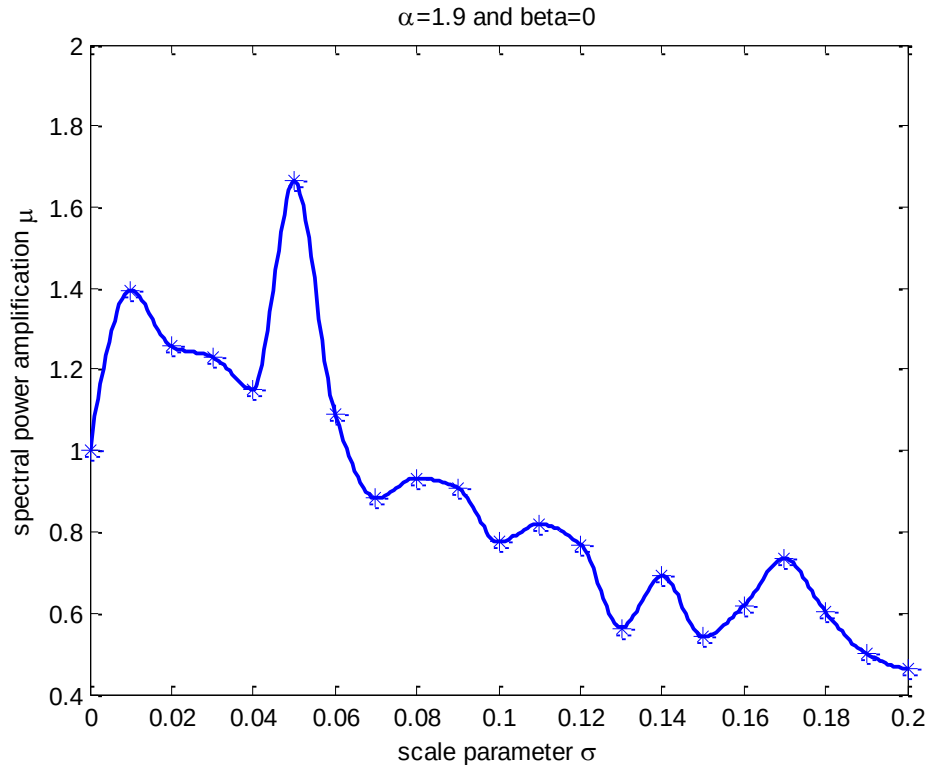

Figure 5.6. The spectral power amplification vs. σ for $\alpha = 1.9$ and $\beta = 0$.

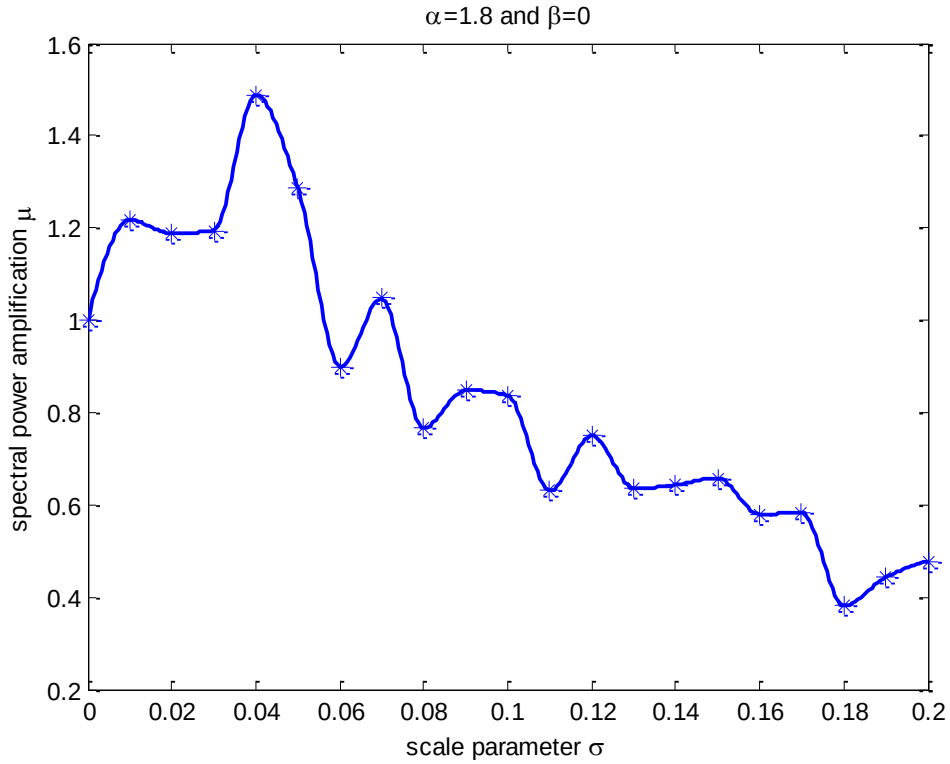

Figure 5.7. The spectral power amplification vs. σ for $\alpha = 1.8$ and $\beta = 0$.

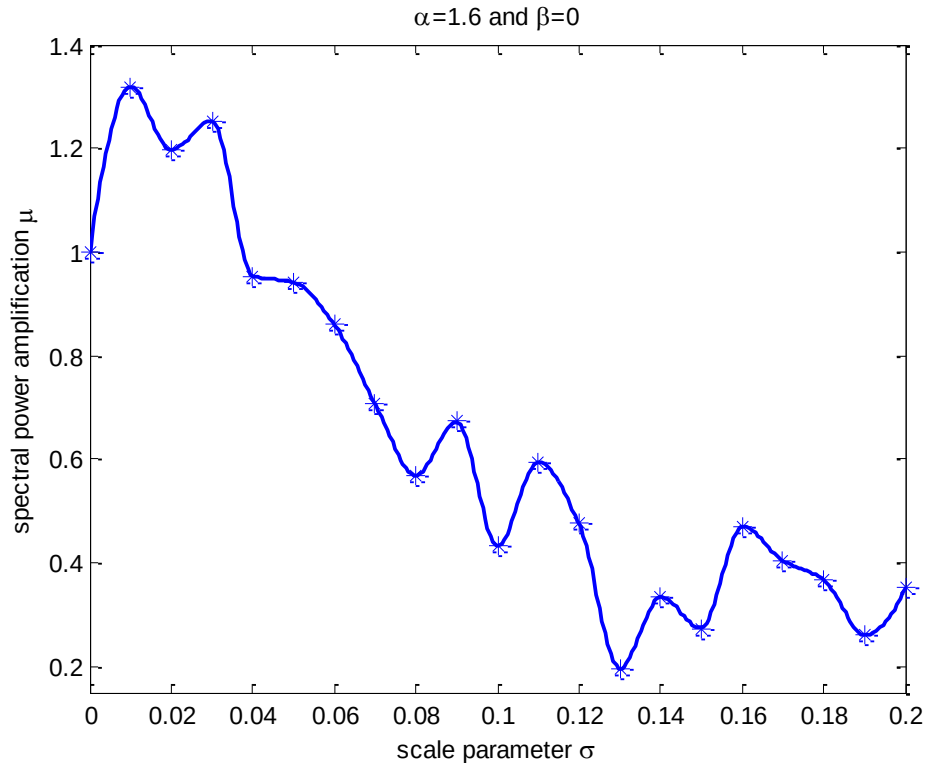

Figure 5.8. The spectral power amplification vs. σ for $\alpha = 1.6$ and $\beta = 0$.

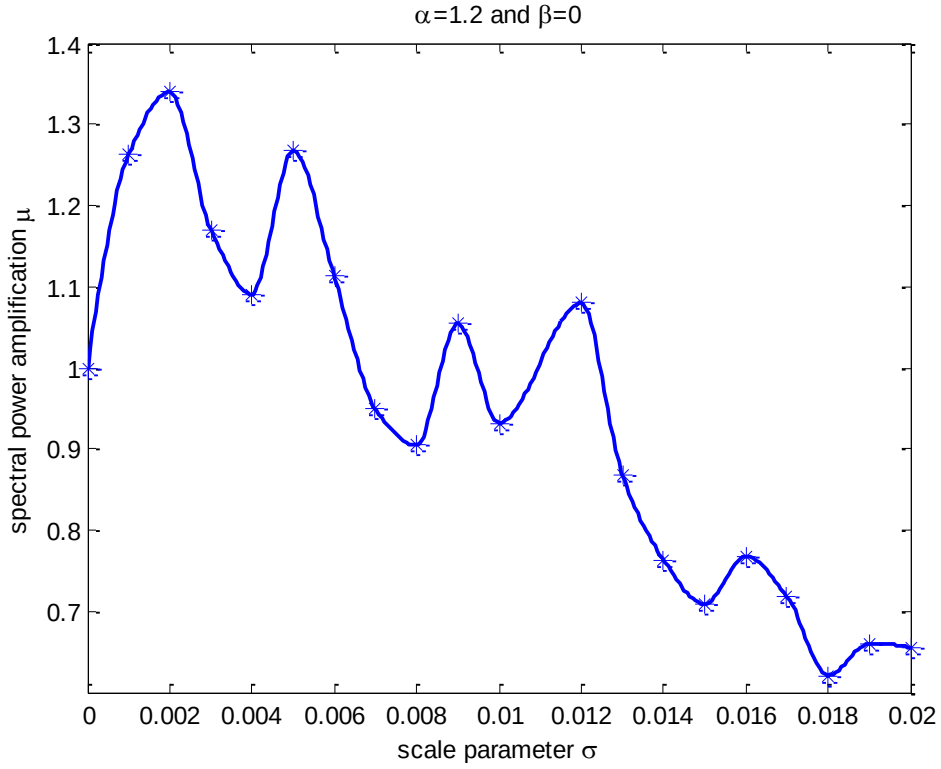

Figure 5.9. The spectral power amplification vs. σ for $\alpha = 1.2$ and $\beta = 0$.

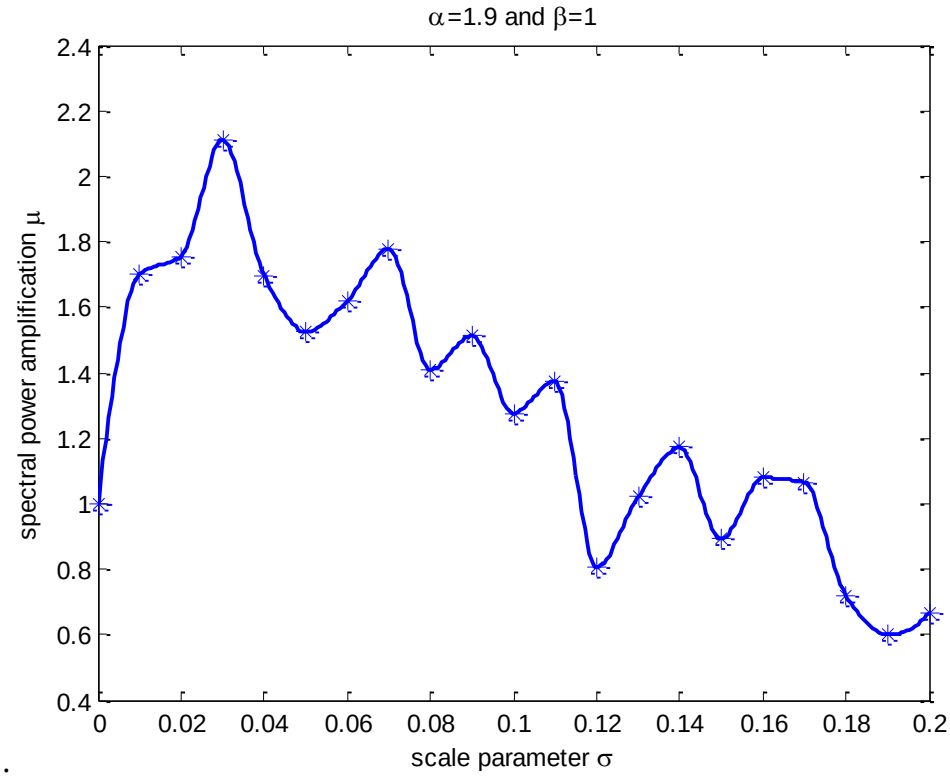

Figure 5.10. The spectral power amplification vs. σ for $\alpha = 1.9$ and $\beta = 1$.

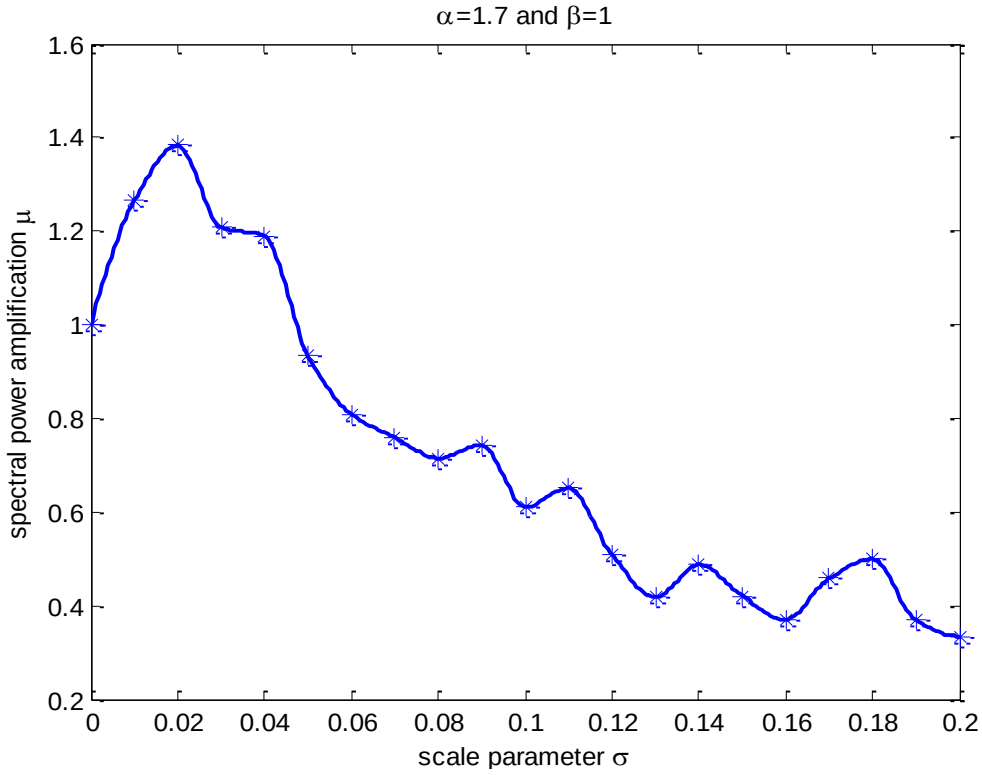

Figure 5.11. The spectral power amplification vs. σ for $\alpha = 1.7$ and $\beta = 1$.

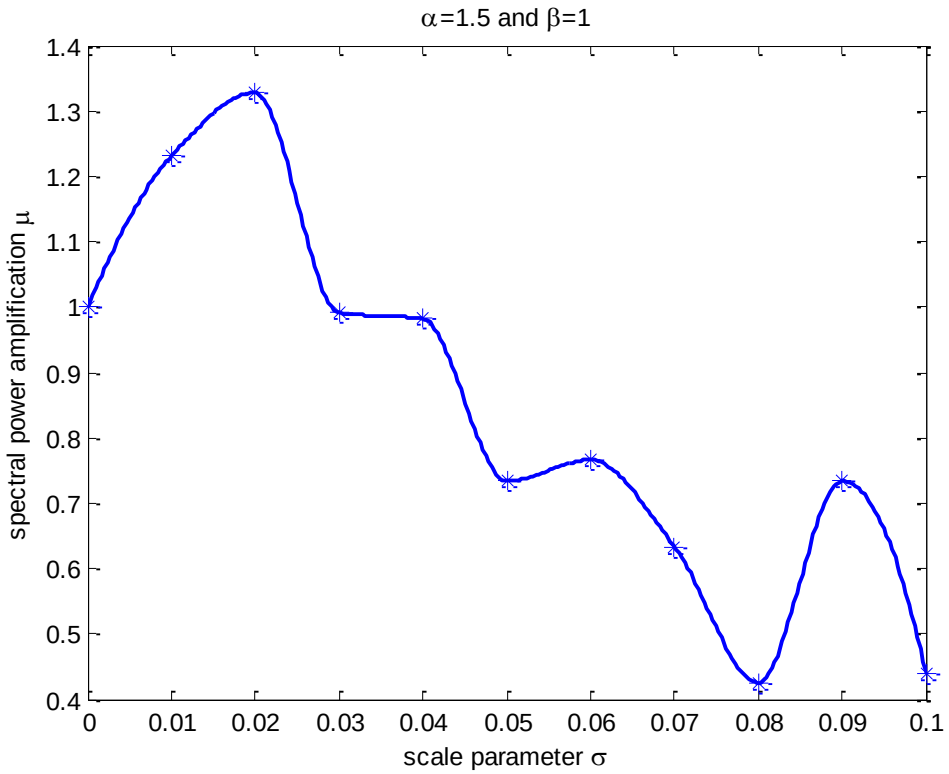

Figure 5.12. The spectral power amplification vs. σ for $\alpha = 1.5$ and $\beta = 1$.

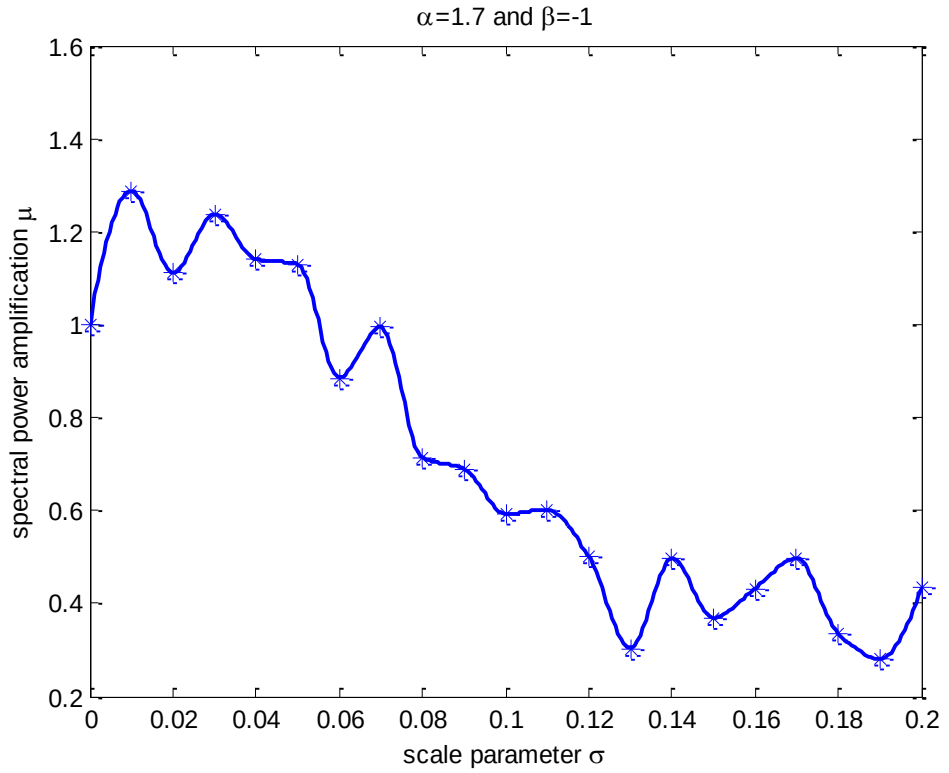

Figure 5.13. The spectral power amplification vs. σ for $\alpha = 1.7$ and $\beta = -1$.

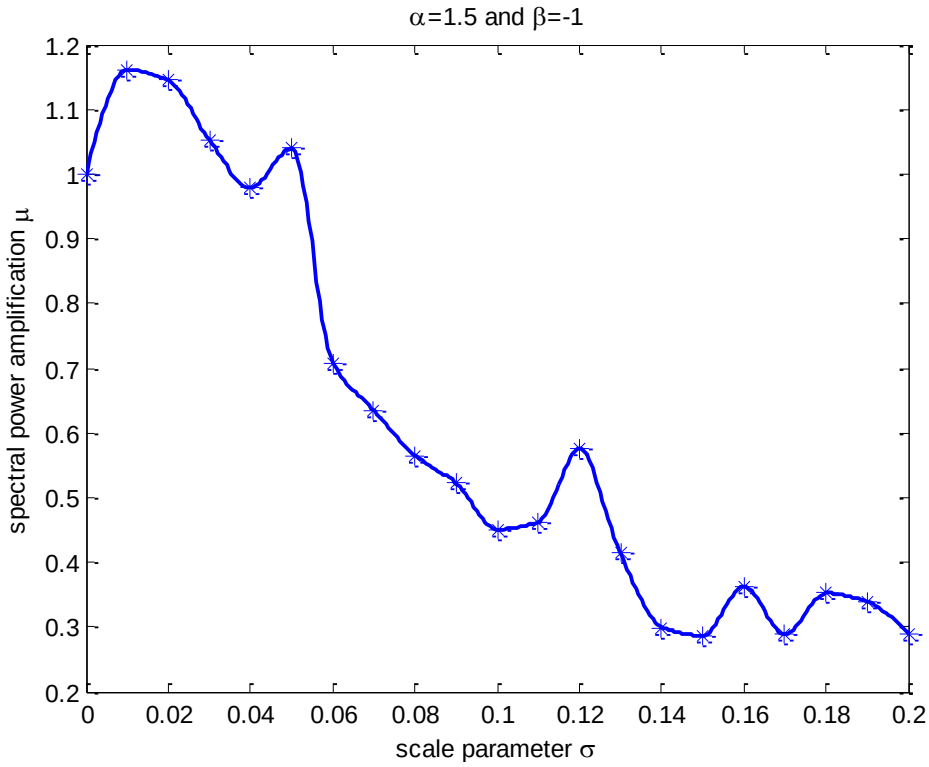

Figure 5.14. The spectral power amplification vs. σ for $\alpha = 1.5$ and $\beta = -1$.

Figure 5.15. shows the relation between characteristic exponent α and scale parameter σ for $\beta = 0,\ \beta = 1$ and $\beta = -1$. For small α values the maximum response occurs at small scale parameter hence σ_{opt} becomes small and for large α values the σ_{opt} increases for all three skewness parameter β. However, in skew-symmetric cases, $\beta = 1$ and $\beta = -1$, the dependence is almost flat for some intermediate α values between 1.2 and 1.9.

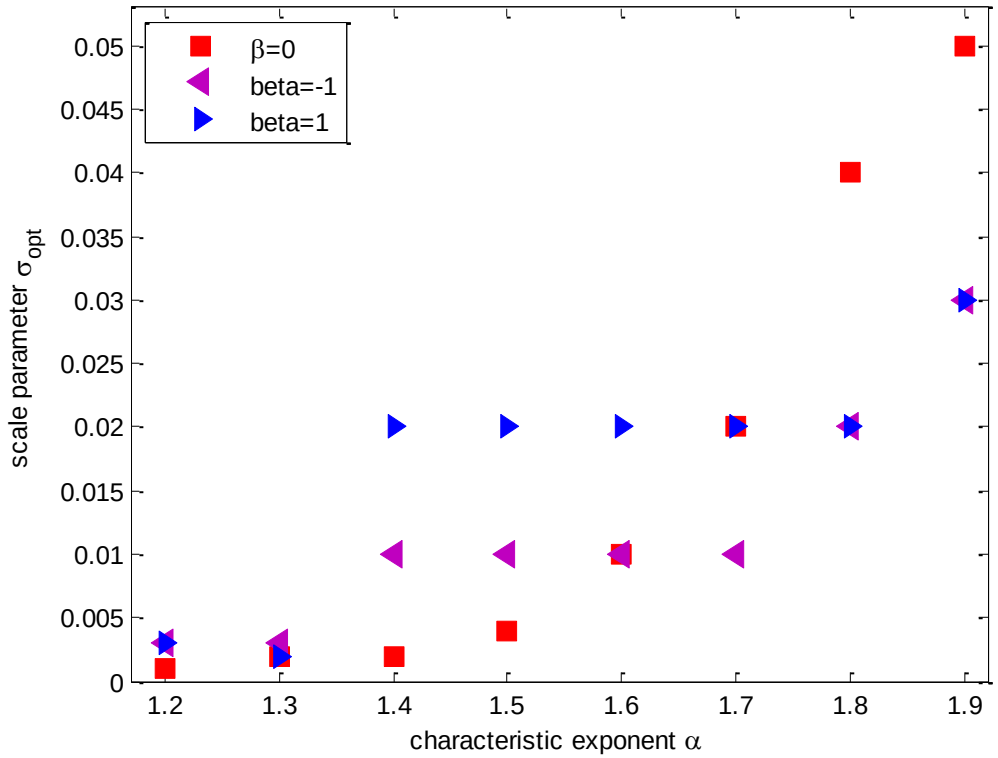

Figure 5.15. The relation between characteristic exponent and scale parameter

The fading effect for $\beta = 0$ can be generalized as an exponential relationship between the optimal noise dispersion γ_{opt} and the characteristic exponent α is shown in Figure 5.16. The γ_{opt} becomes smaller as the noise becomes more impulsive. The relation between dispersion and scale parameter is given as seen in Chapter 3.1.

For skew-symmetric cases the relation between the optimal noise dispersion γ_{opt} and the characteristic exponent α is shown as in Figures 5.17-5.18. From the figures it can be observed that for some α values the relation provides a resonance effect.

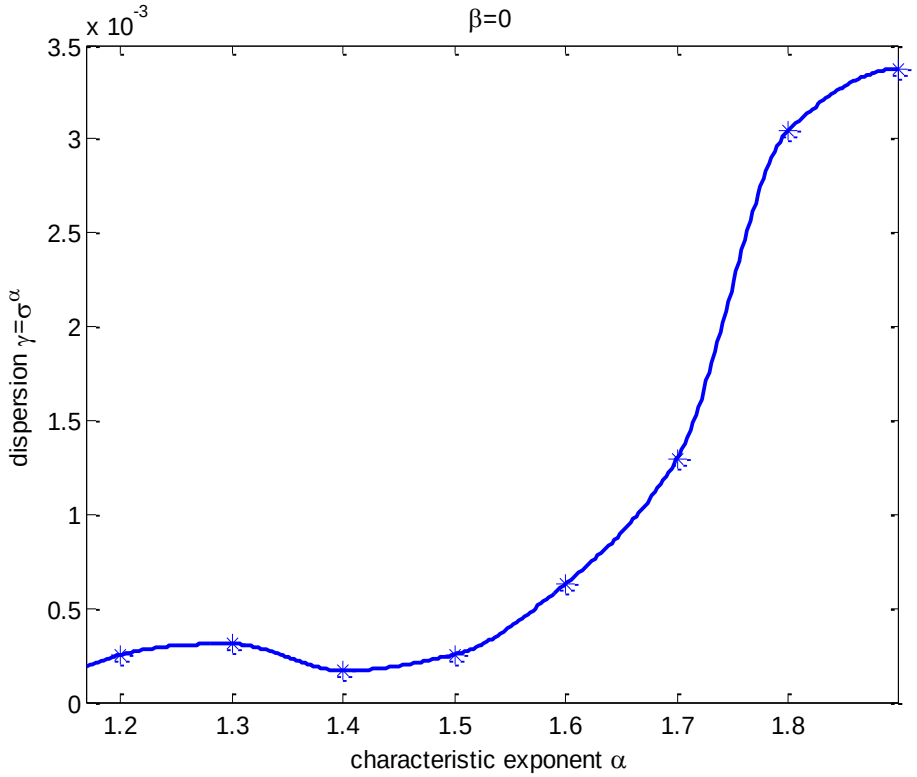

Figure 5.16. Exponential law for γ_{opt} and α for $\beta = 0$.

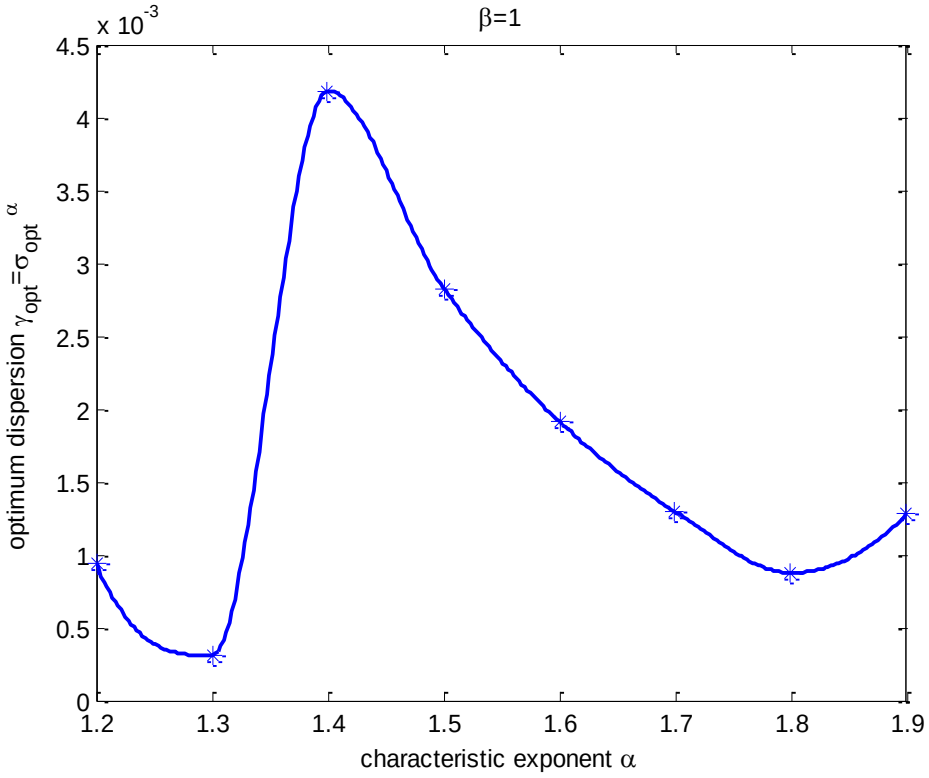

Figure 5.17. The relation between γ_{opt} and α for $\beta = 1$.

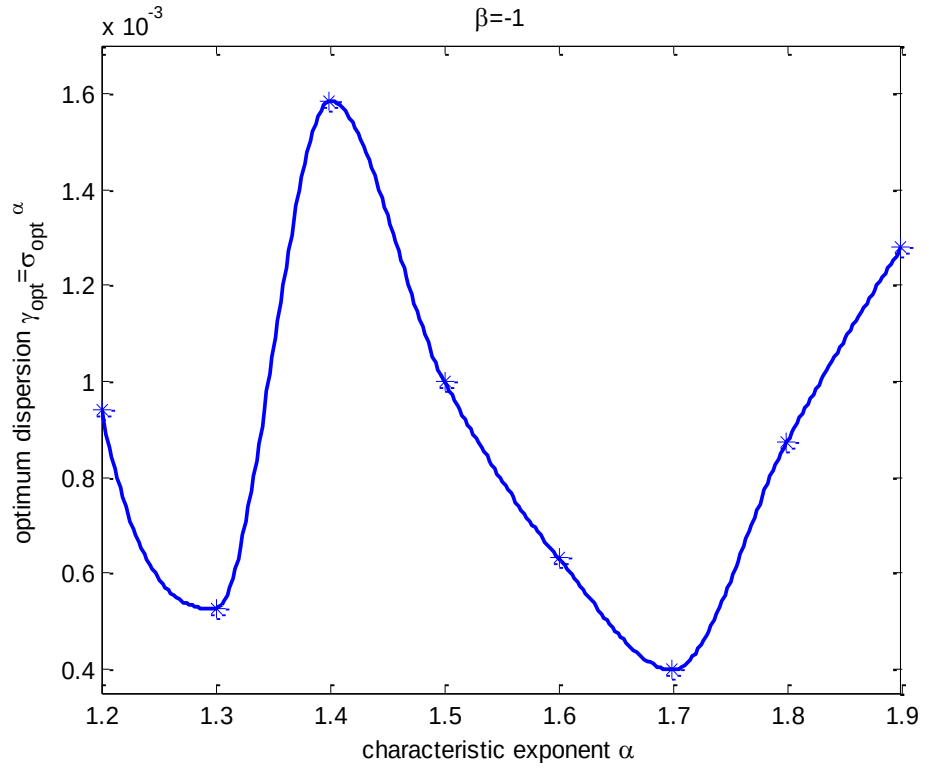

Figure 5.18. The relation between γ_{opt} and α for $\beta = -1$.

Figures 5.19 and 5.21 show the effect of noise parameter skewness with $\beta = 0,\ \beta = 1$ and $\beta = -1$, respectively.

The two-state process which takes into account only transitions between the attractors and ignores the detailed motion within each attractor, denoted by $\theta(t)$ takes values only ± 1 depending on the selected attractor as either below or above the specified threshold level. The threshold level for crossing is chosen as 1 V.

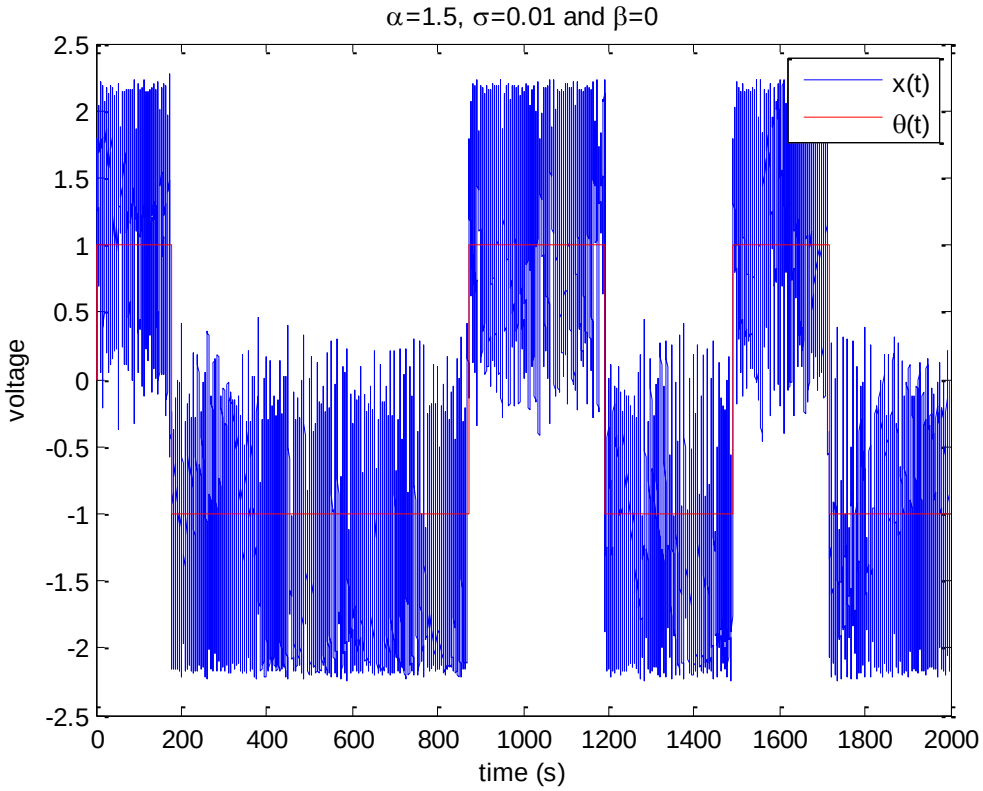

Figure 5.19. Trajectories of the output with $\beta = -1$

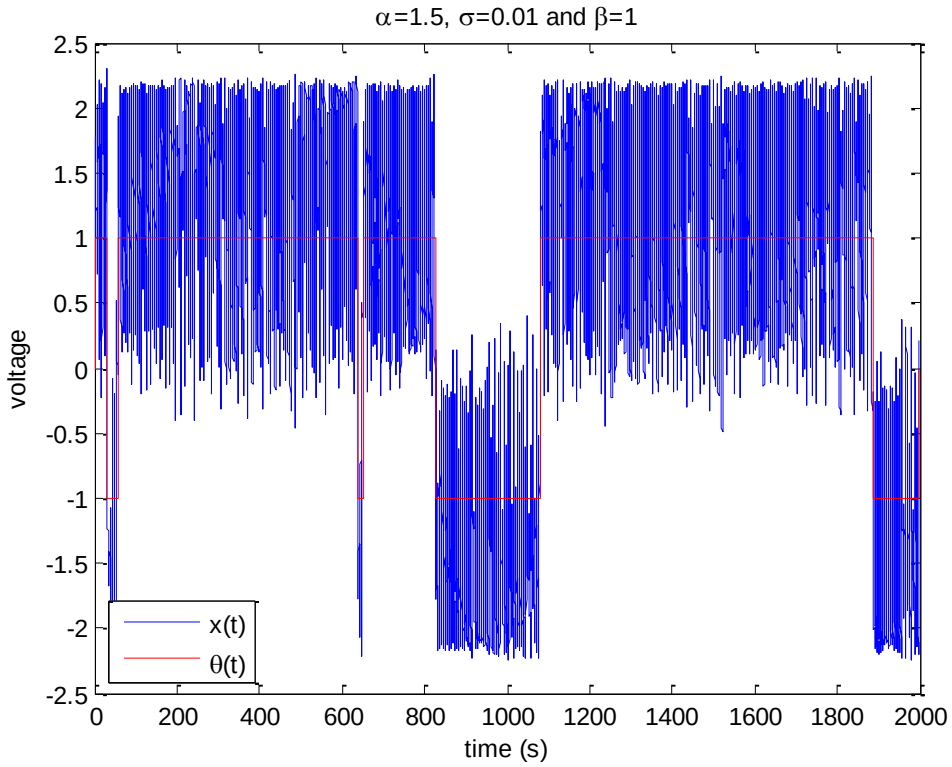

Figure 5.20. Trajectories of the output with $\beta = 1$

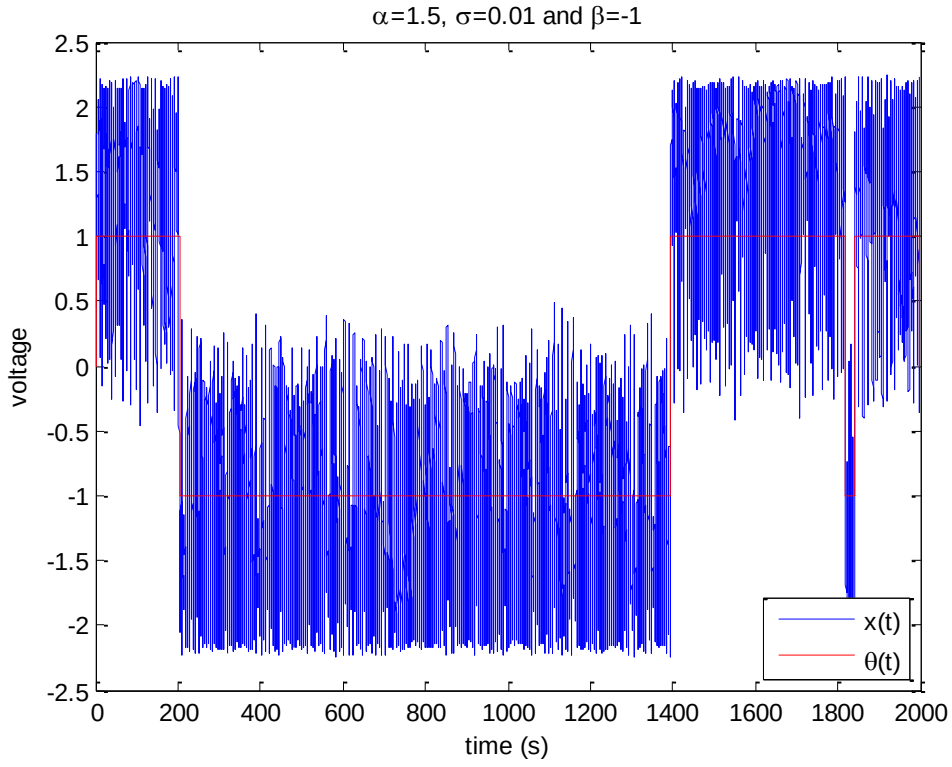

Figure 5.21. Trajectories of the output with $\beta = -1$.

Beginning with the Gaussian noise which is special case of α-stable noise ($\alpha = 2$) Figures 5.22-5.27 show the variation of the mean residence time as a function of scale parameter of noise σ for the skew symmetric case ($\beta = 1$).

Two-state dynamics have been used to compute the MRs in a selected attractor i.e. upper scroll attractor in our case. The results have been averaged for a set of 100 residence times.

As α decreases, MRs also decrease as a function of scale parameter σ. On the other hand, as scale parameter σ increases for each α value, MRs first increase and then decrease.

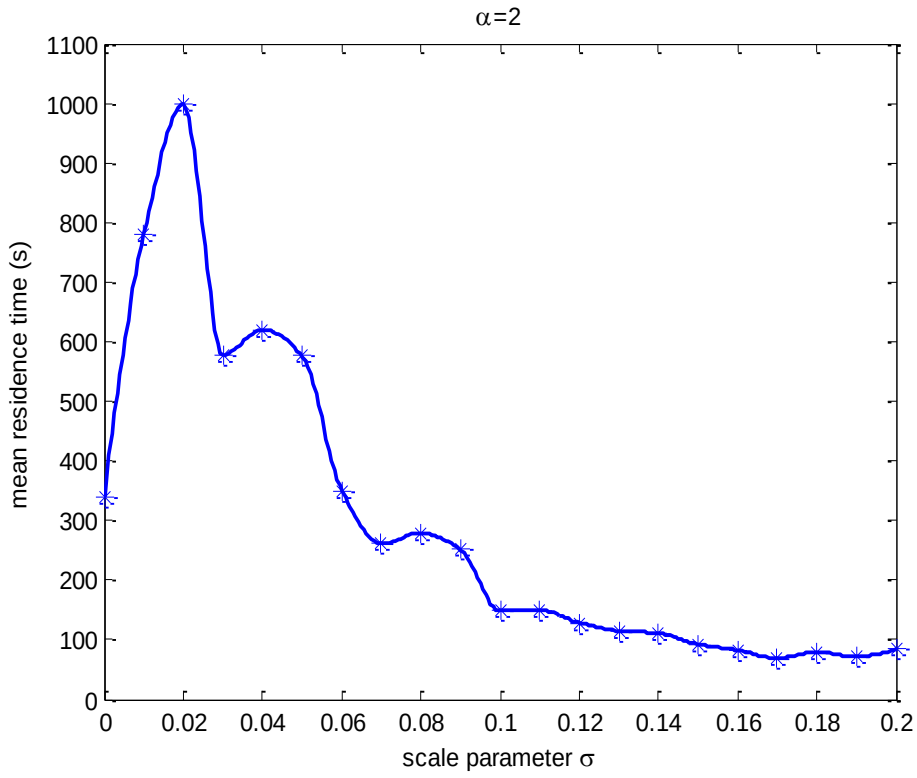

Figure 5.22. Mean residence time vs. scale parameter σ for Gaussian case.

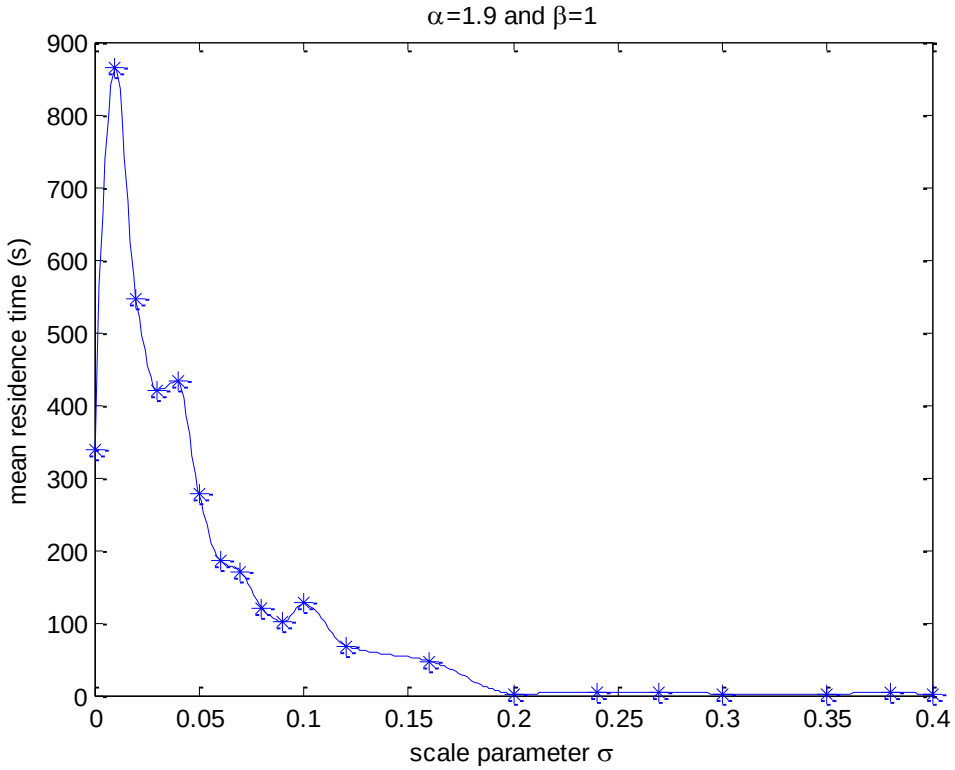

Figure 5.23. Mean residence time vs. scale parameter σ for α=1.9

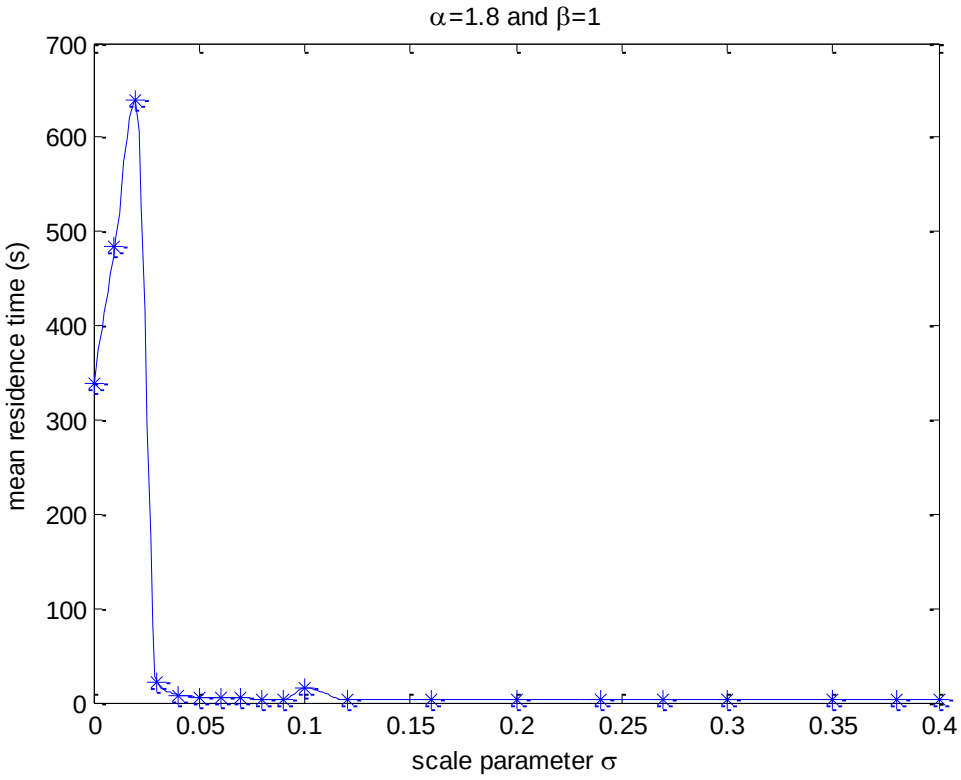

Figure 5.24. Mean residence time vs. scale parameter σ for α=1.8

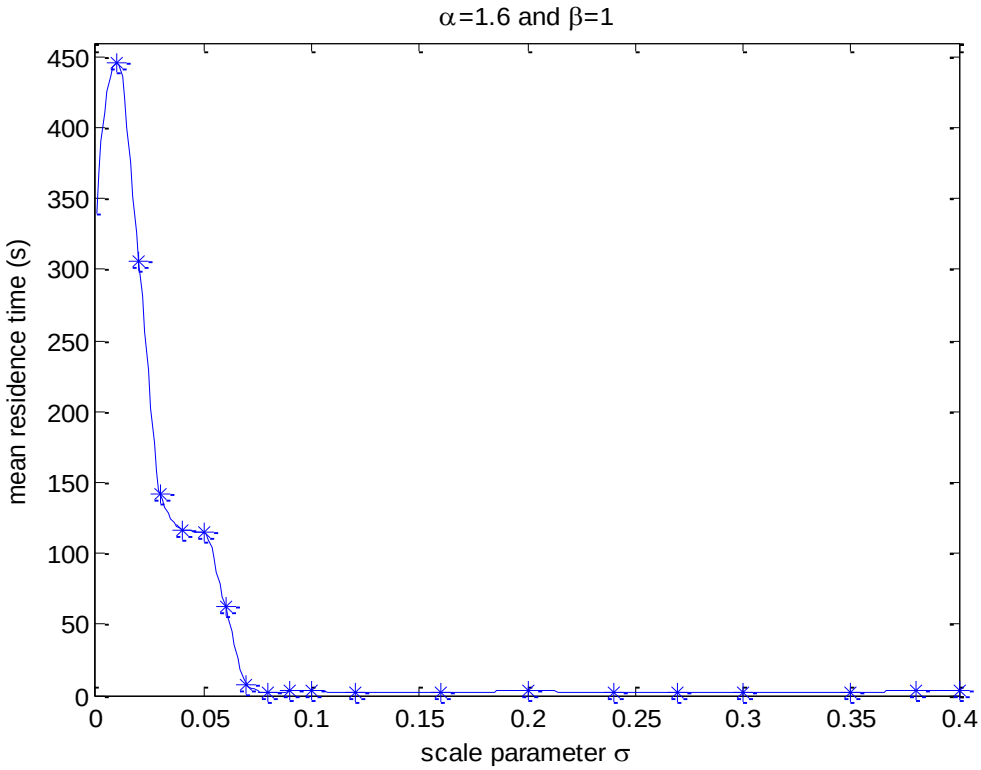

Figure 5.25. Mean residence time vs. scale parameter σ for α=1.6

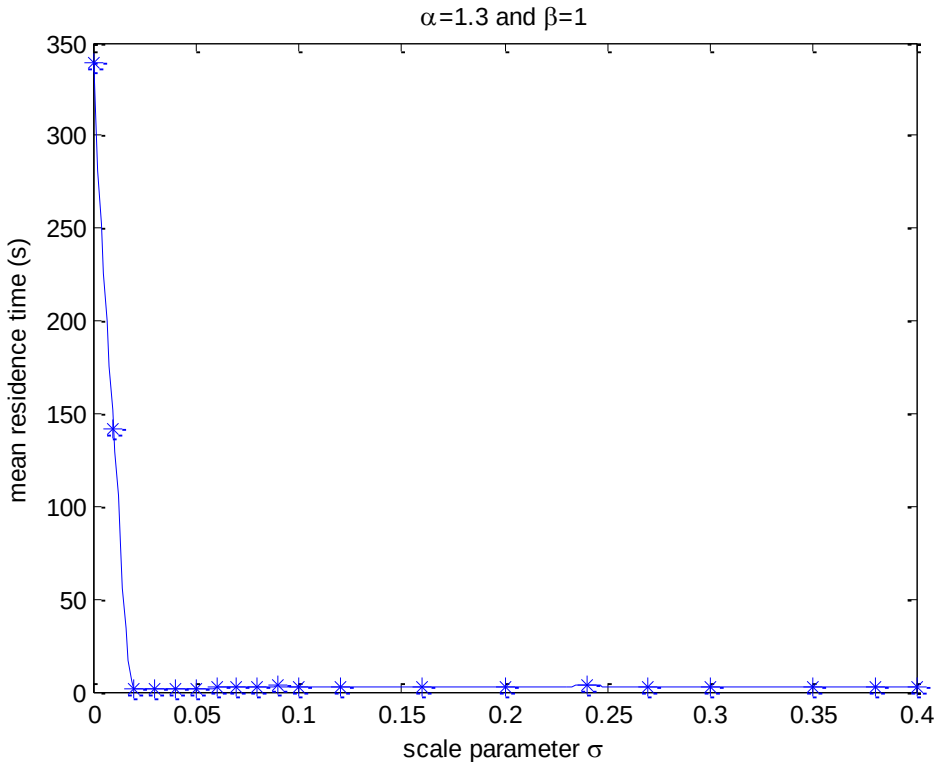

Figure 5.26. Mean residence time vs. scale parameter σ for α=1.3

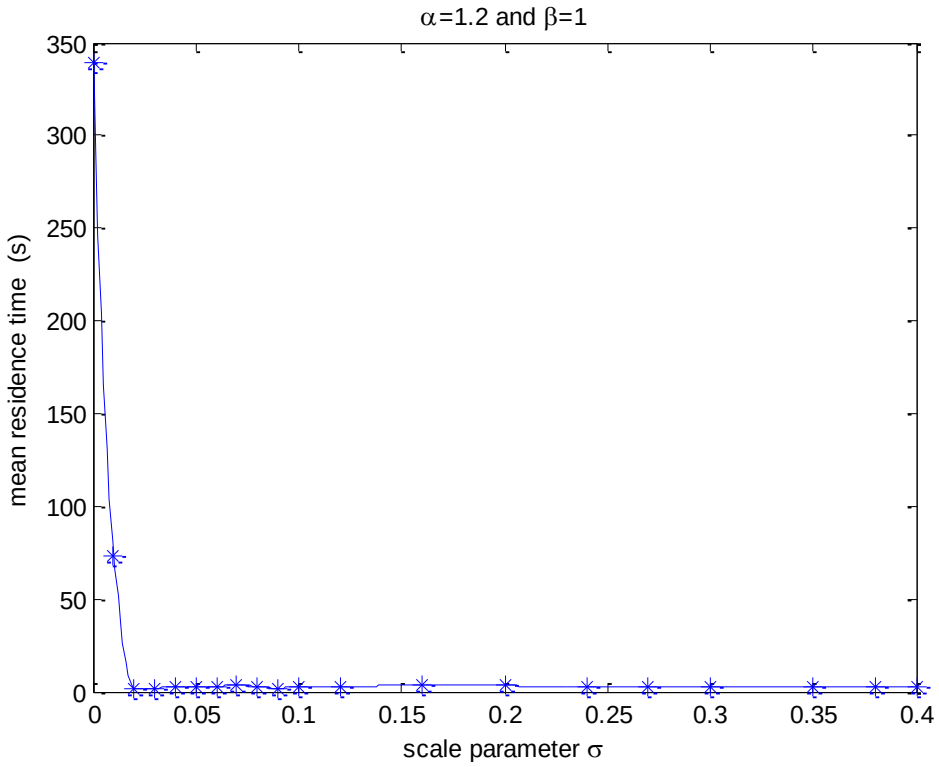

Figure 5.27. Mean residence time vs. scale parameter σ for α=1.2

The mean residence times in a single-scroll attractor for a specified characteristic exponent (i.e. $\alpha = 1.6$) and for symmetric and skew-symmetric noise distributions, $\beta = 0,\ 1, -1$ are shown as seen in Figure 5.28. MRs first increase and then decrease as a function of scale parameter.

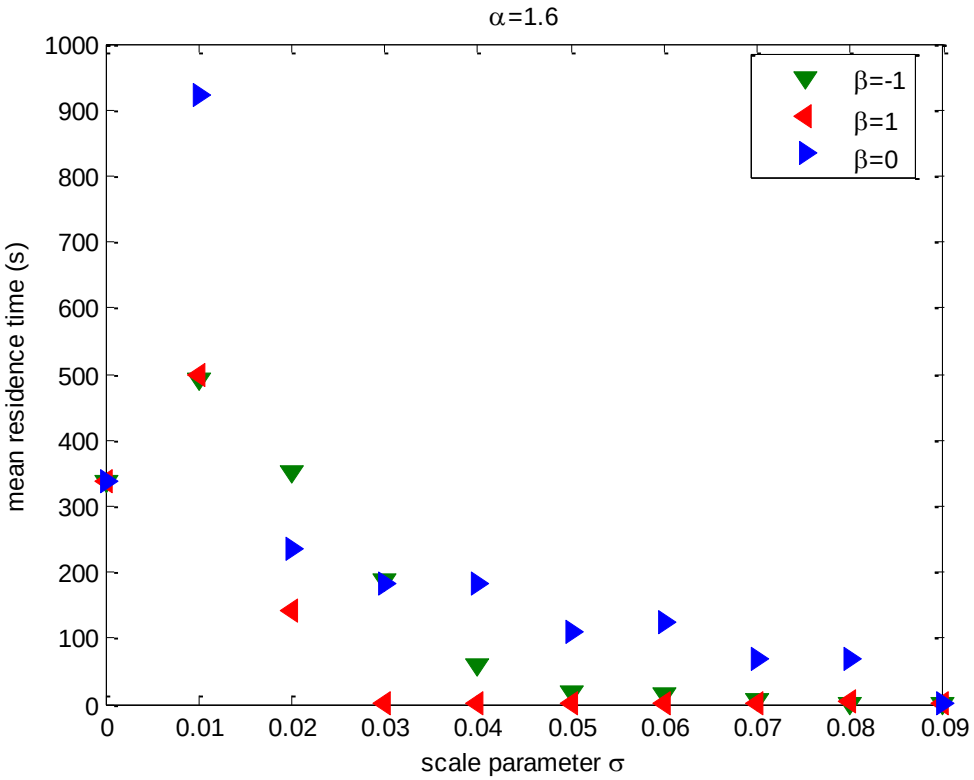

Figure 5.28. Mean residence time vs. σ for α=1.6 with $\beta = 0, 1$ and -1

The mean residence time for various characteristic exponents in the case $\beta = 0, 1 \text{ and } -1$ is shown as in Figure 5.29, 5.30 and 5.31, respectively. When α becomes larger mean residence time also becomes larger for symmetric and skew-symmetric cases.

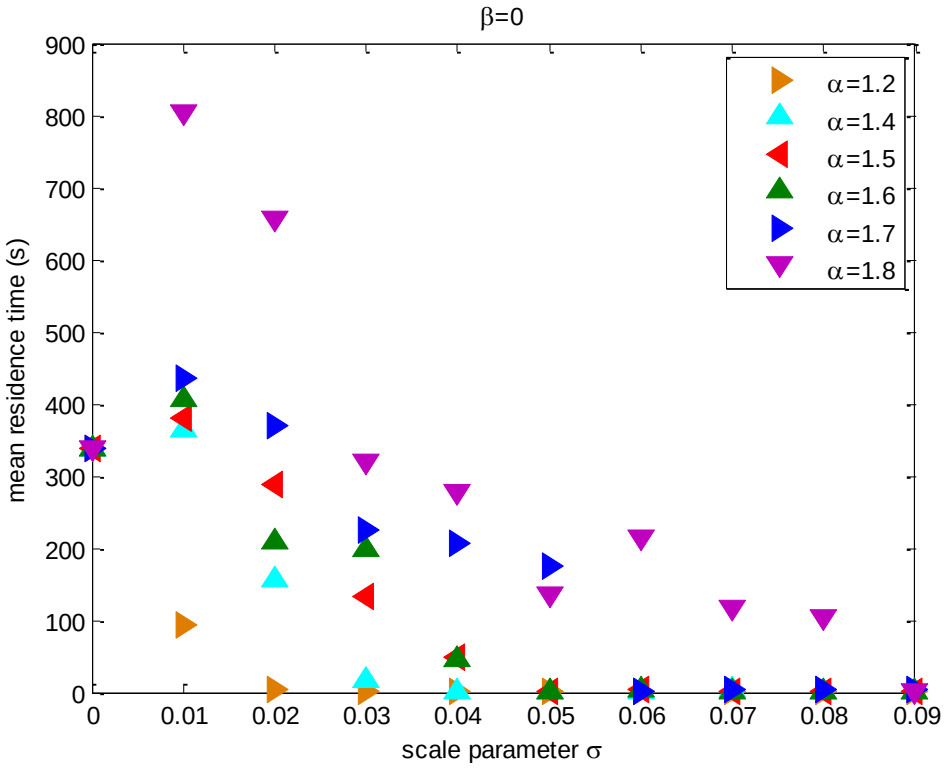

Figure 5.29. Mean residence time vs. scale parameter σ for various α and β=0.

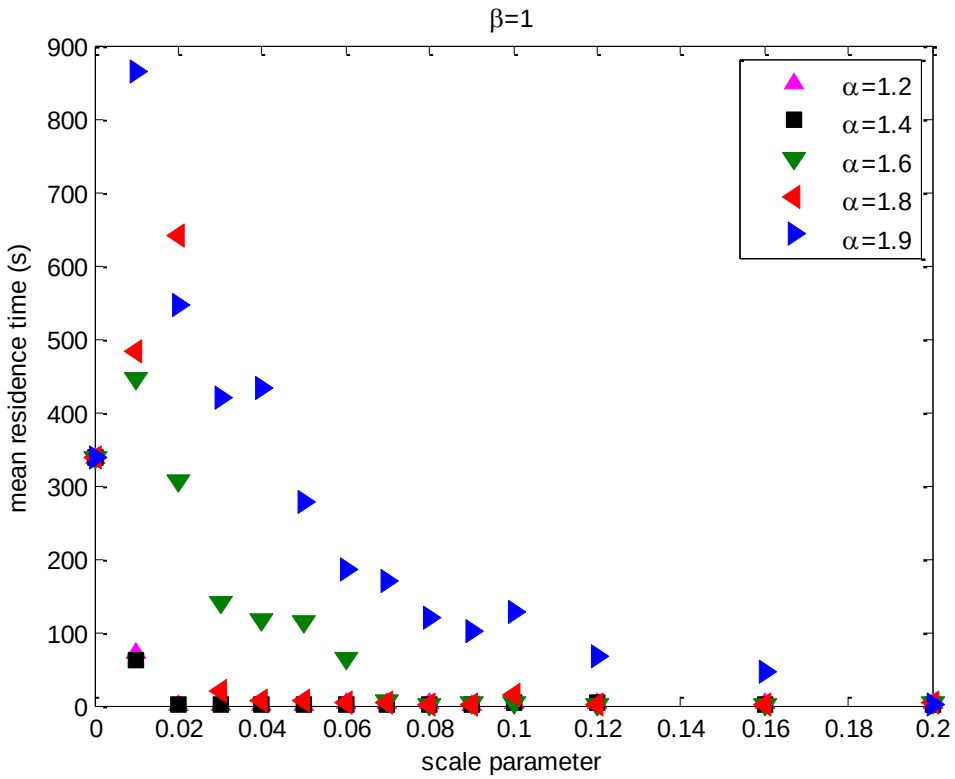

Figure 5.30. Mean residence time vs. scale parameter σ for various α and β=1.

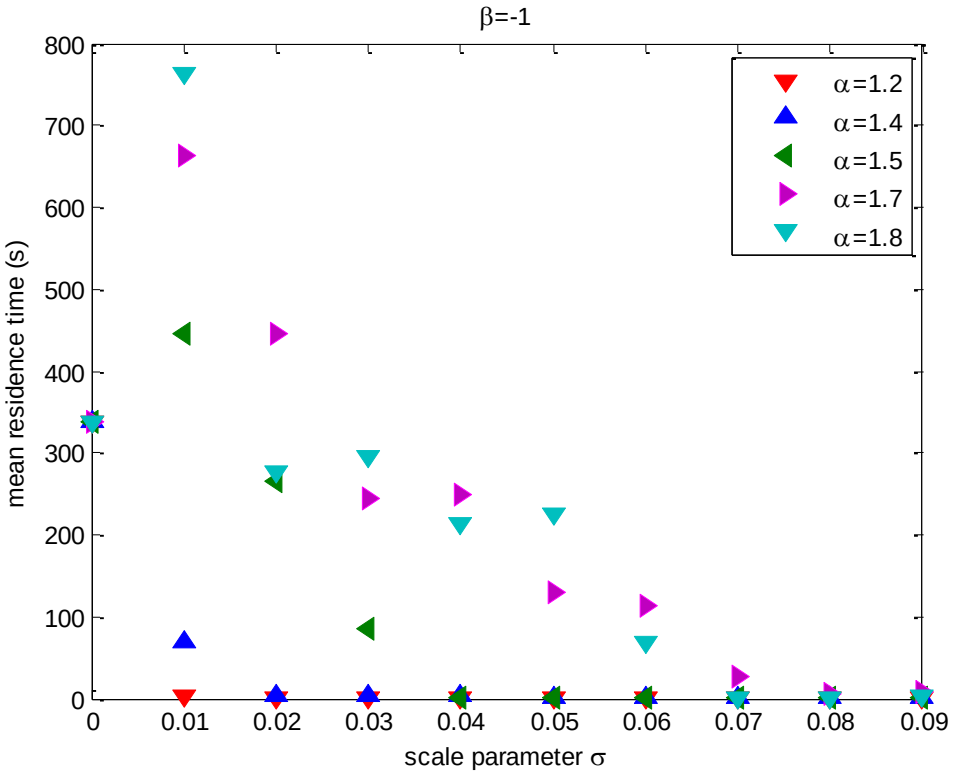

Figure 5.31. Mean residence time vs. scale parameter σ for various α and β=-1.

The mean residence times for various characteristic exponents α for a specified σ are shown as in Figure 5.32. MRs decrease when noise becomes more impulsive for both symmetric ($\beta = 0$) and skew-symmetric cases (i.e. $\beta = \mp 1$). From the Figure 5.32 it can be seen that with the increase of α MR increases however, when $\alpha = 2$ (Gaussian case) mean residence time decreases.

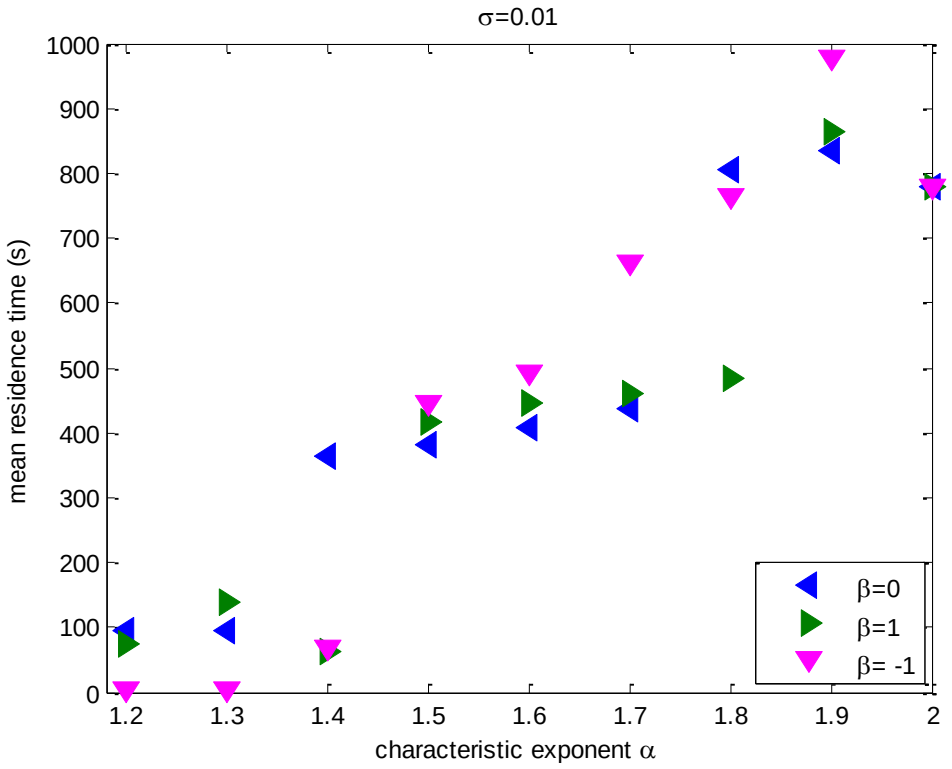

Figure 5.32. Mean residence time vs. α for σ=0.01.

CHAPTER 6

CONCLUSION

In this thesis, we studied the stochastic resonance in Chua's circuit driven by alpha-stable noise. We first determined a threshold value for the amplitude of input periodic signal as a function of its frequency to ensure that it could not induce jumps between the attractors in the absence of noise. Then the response of system in the presence of noise was evaluated through fractional low order Wigner Ville distribution in the framework of spectral power amplification as a measure of SR. All simulations have shown a visible stochastic resonance (SR) effect in Chua's circuit driven by α-stable noise with β=0, 1 and also-1. Simulation results also show multiple maxima as a function of noise scale parameter. It has been observed that the optimum noise dispersion in the case that SPA has a maximum decreases as the noise distribution becomes more impulsive. The maximum of amplification factor decreases with decreasing characteristic exponent for symmetric case. Hence the SR effect fades as the noise grows more impulsive. In skew- symmetric cases for some characteristic exponent α values the relation between the optimal noise dispersion and α provides a resonance effect.

Another aim of this thesis is to analyze the effect of noise parameters on lifetime of a trajectory spent in an attractor. By investigating the mean residence times it has been observed that when α decreases, MRs also decrease as a function of scale parameter σ. On the other hand, as scale parameter σ increases for small α values (i.e. a=1.2, 1.3), MRs decrease whereas for α values between the 1.3 and 2, MRs first increase and then decrease.

As a further study Chua's circuit driven by α-stable noise can be implemented in Field Programmable Gate Array (FPGA) to use in secure digital chaotic communication system. The performance of sensor network i.e. olfactory system can be enhanced by the addition of an optimum amount noise.

REFERENCES

Altınkaya, M. A., H. Deliç, et al. (2002). "Subspace-based frequency estimation of sinusoidal signals in alpha-stable noise." Signal processing **82**(12): 1807-1827.

Anishchenko, V., A. Neiman, et al. (1993). "Stochastic resonance in chaotic systems." Journal of statistical physics **70**(1): 183-196.

Anishchenko, V. and M. Safonova (1992). "Stochastic resonance in chua's circuit." INT. J. BIFURCATION CHAOS. **2**(2): 397-401.

Anishchenko, V. and M. Safonova (1994). "Stochastic resonance in Chua's circuit driven by amplitude or frequency modulated signals." International Journal of Bifurcation and Chaos in Applied Sciences and Engineering **4**(2): 441-446.

Anishchenko, V. S., A. B. Neiman, et al. (1999). "Stochastic resonance: noise-enhanced order." Physics-Uspekhi **42**: 7.

Bahar, S. and F. Moss (2003). "The Nonlinear Dynamics of the Crayfish Mechanoreceptor System." International Journal of Bifurcation and Chaos in Applied Sciences and Engineering **13**(8): 2013-2034.

Barbay, S., G. Giacomelli, et al. (2000). "Experimental evidence of binary aperiodic stochastic resonance." Physical Review Letters **85**(22): 4652-4655.

Benzi, R., G. Parisi, et al. (1982). "Stochastic resonance in climatic change." Tellus **34**(1): 10-16.

Benzi, R., G. Parisi, et al. (1983). "A theory of stochastic resonance in climatic change." SIAM Journal on applied mathematics: 565-578.

Benzi, R., A. Sutera, et al. (1981). "The mechanism of stochastic resonance." Journal of Physics A: mathematical and general **14**: L453.

Bulsara, A. R. and A. Zador (1996). "Threshold detection of wideband signals: A noise-induced maximum in the mutual information." Physical Review E **54**(3): 2185-2188.

Chiang, H. H. and C. Nikias (1990). "A new method for adaptive time delay estimation for non-Gaussian signals." Acoustics, Speech and Signal Processing, IEEE Transactions on **38**(2): 209-219.

Chua, L. O., C. W. Wu, et al. (1993). "A universal circuit for studying and generating chaos. I. Routes to chaos." Circuits and Systems I: Fundamental Theory and Applications, IEEE Transactions on **40**(10): 732-744.

Collins, J., C. C. Chow, et al. (1995). "Aperiodic stochastic resonance in excitable systems." Physical Review E **52**(4): 3321-3324.

Collins, J., C. C. Chow, et al. (1995). "Stochastic resonance without tuning." Nature **376**(6537): 236-238.

Collins, J. J., T. T. Imhoff, et al. (1996). "Noise-enhanced tactile sensation." Nature; Nature.

Cuomo, K. M. and A. V. Oppenheim (1993). "Circuit implementation of synchronized chaos with applications to communications." Physical Review Letters **71**(1): 65-68.

Djeddi, M. and M. Benidir (2004). Robust polynomial Wigner-Ville distribution for the analysis of polynomial phase signals in α-stable noise, IEEE.

Douglass, J. K., L. Wilkens, et al. (1993). "Noise enhancement of information transfer in crayfish mechanoreceptors by stochastic resonance." Nature **365**(6444): 337-340.

Dybiec, B. and E. Gudowska-Nowak (2006). "Stochastic resonance: The role of alpha-stable noises." ACTA PHYSICA POLONICA SERIES B **37**(5): 1479.

Dybiec, B. and E. Gudowska-Nowak (2009). "Lévy stable noise-induced transitions: stochastic resonance, resonant activation and dynamic hysteresis." Journal of Statistical Mechanics: Theory and Experiment **2009**: P05004.

Freund, J. A., L. Schimansky-Geier, et al. (2002). "Behavioral stochastic resonance: how the noise from a Daphnia swarm enhances individual prey capture by juvenile paddlefish." Journal of theoretical biology **214**(1): 71-83.

Gammaitoni, L., P. Hänggi, et al. (1998). "Stochastic resonance." Reviews of Modern Physics **70**(1): 223.

Gammaitoni, L., F. Marchesoni, et al. (1995). "Stochastic resonance as a bona fide resonance." Physical Review Letters **74**(7): 1052-1055.

Gang, H., T. Ditzinger, et al. (1993). "Stochastic resonance without external periodic force." Physical Review Letters **71**(6): 807-810.

Genesio, R. and A. Tesi (1991). Chaos prediction in nonlinear feedback systems, IET.

Genesio, R. and A. Tesi (1992). "A harmonic balance approach for chaos prediction: Chua's circuit." Int. J. Bifurcation Chaos **2**(1): 61-79.

Gomes, I., C. R. Mirasso, et al. (2003). "Experimental study of high frequency stochastic resonance in Chua circuits." Physica A: Statistical Mechanics and its Applications **327**(1): 115-119.

Gotz, M., U. Feldmann, et al. (1993). "Synthesis of higher dimensional Chua circuits." Circuits and Systems I: Fundamental Theory and Applications, IEEE Transactions on **40**(11): 854-860.

Griffith Jr, D. W., J. G. Gonzalez, et al. (1997). Robust time-frequency representations for signals in α-stable noise using fractional lower-order statistics, IEEE.

He, D., Y. Lin, et al. (2010). "A novel spectrum-sensing technique in cognitive radio based on stochastic resonance." Vehicular Technology, IEEE Transactions on **59**(4): 1680-1688.

Janicki, A. and A. Weron (1994). Simulation and chaotic behavior of α-stable stochastic processes, CRC.

Jiang, J., T. Huang, et al. (2010). Pseudo-Power Spectrum Estimation Method Based on Fractional Low-Order Covariance Matrix. E-Product E-Service and E-Entertainment (ICEEE), 2010 International Conference on.

Jiang, J. L. and D. F. Zha (2008). Generalized fractional lower-order spectrum of alpha stable distribution process, IEEE.

Jung, P. and P. Hänggi (1991). "Amplification of small signals via stochastic resonance." Physical review A **44**(12): 8032-8042.

Kay, S., J. H. Michels, et al. (2006). "Reducing probability of decision error using stochastic resonance." Signal Processing Letters, IEEE **13**(11): 695-698.

Korneta, W., I. Gomes, et al. (2006). "Experimental study of stochastic resonance in a Chua's circuit operating in a chaotic regime." Physica D: Nonlinear Phenomena **219**(1): 93-100.

Kosko, B. and S. Mitaim (2001). "Robust stochastic resonance: Signal detection and adaptation in impulsive noise." Physical Review E **64**(5): 051110.

Kosko, B. and S. Mitaim (2003). "Stochastic resonance in noisy threshold neurons." Neural Networks **16**(5-6): 755-761.

Kurita, Y., M. Shinohara, et al. (2011). Wearable sensorimotor enhancer for a fingertip based on stochastic resonance, IEEE.

Kuruoglu, E. E. (2001). "Density parameter estimation of skewed α-stable distributions." Signal Processing, IEEE Transactions on **49**(10): 2192-2201.

Leonard, D. S. and L. Reichl (1994). "Stochastic resonance in a chemical reaction." Physical Review E **49**(2): 1734.

Longtin, A. (1993). "Stochastic resonance in neuron models." Journal of statistical physics **70**(1): 309-327.

Lugo, E., R. Doti, et al. (2008). "Ubiquitous crossmodal stochastic resonance in humans: auditory noise facilitates tactile, visual and proprioceptive sensations." PLoS One **3**(8): e2860.

Ma, X. and C. L. Nikias (1995). "Parameter estimation and blind channel identification in impulsive signal environments." Signal Processing, IEEE Transactions on **43**(12): 2884-2897.

Ma, X. and C. L. Nikias (1996). "Joint estimation of time delay and frequency delay in impulsive noise using fractional lower order statistics." Signal Processing, IEEE Transactions on **44**(11): 2669-2687.

Marks, R. J., B. Thompson, et al. (2002). Stochastic resonance of a threshold detector: image visualization and explanation, IEEE.

McDonnell, M. D., N. G. Stocks, et al. (2008). "Stochastic resonance: from suprathreshold stochastic resonance to stochastic signal quantization."

McNamara, B. and K. Wiesenfeld (1989). "Theory of stochastic resonance." Physical review A **39**(9): 4854.

Morse, R. P. and E. F. Evans (1996). "Enhancement of vowel coding for cochlear implants by addition of noise." Nature medicine **2**(8): 928-932.

Morse, R. P. and P. Roper (2000). "Enhanced coding in a cochlear-implant model using additive noise: Aperiodic stochastic resonance with tuning." Physical Review E **61**(5): 5683.

Moss, F., L. M. Ward, et al. (2004). "Stochastic resonance and sensory information processing: a tutorial and review of application." Clinical Neurophysiology **115**(2): 267-281.

Nikias, C. L. and M. Shao (1995). Signal processing with alpha-stable distributions and applications, Wiley-Interscience.

Özkurt, N. (2004). Synthesis of Nonlinear Circuits in Time-Frequency Domain. Electrical and Electronics Engineering, Dokuz Eylül University.

Palenzuela, C., R. Toral, et al. (2001). "Coherence resonance in chaotic systems." EPL (Europhysics Letters) **56**: 347.

Parker, T. S. and L. O. Chua (1987). "Chaos: A tutorial for engineers." Proceedings of the IEEE **75**(8): 982-1008.

Parlitz, U., L. Chua, et al. (1992). "Experimental demonstration of secure communications via chaotic synchronization." Int JBC **2**(3): 709-713.

Pecora, L. M. and T. L. Carroll (1990). "Synchronization in chaotic systems." Physical Review Letters **64**(8): 821-824.

Peng, R., H. Chen, et al. (2009). "Noise-enhanced detection of micro-calcifications in digital mammograms." Selected Topics in Signal Processing, IEEE Journal of **3**(1): 62-73.

Priplata, A. A., J. B. Niemi, et al. (2003). "Vibrating insoles and balance control in elderly people." The Lancet **362**(9390): 1123-1124.

Priplata, A. A., B. L. Patritti, et al. (2006). "Noise-enhanced balance control in patients with diabetes and patients with stroke." Annals of neurology **59**(1): 4-12.

Richardson, K. A., T. T. Imhoff, et al. (1998). "Using electrical noise to enhance the ability of humans to detect subthreshold mechanical cutaneous stimuli." Chaos **8**(3): 599-603.

Russell, D. F., L. A. Wilkens, et al. (1999). "Use of behavioural stochastic resonance by paddle fish for feeding." Nature **402**(6759): 291-293.

Samorodnitsky, G. and M. Taqqu "Stable Non-Gaussian Random Processes. 1994." Chapman&Hall, New York.

Schiff, S. J., K. Jerger, et al. (1994). "Controlling chaos in the brain." Nature **370**(6491): 615-620.

Shanmugan, K. S. and A. M. Breipohl (1988). "Random signals: detection, estimation, and data analysis."

Shao, M. and C. L. Nikias (1993). "Signal processing with fractional lower order moments: Stable processes and their applications." Proceedings of the IEEE **81**(7): 986-1010.

Söderlund, G. B. W., S. Sikström, et al. (2010). "The effects of background white noise on memory performance in inattentive school children." Behavioral and Brain Functions **6**(1): 55.

Stocks, N. (2000). "Suprathreshold stochastic resonance in multilevel threshold systems." Physical Review Letters **84**(11): 2310-2313.

Stocks, N. G., D. Allingham, et al. (2002). "The application of suprathreshold stochastic resonance to cochlear implant coding." Fluctuation and Noise Letters **2**(3): L169-L181.

Stotland, A. and M. Di Ventra (2011). "Stochastic memory: memory enhancement due to noise." Arxiv preprint arXiv:1104.4485.

Strogatz, S. H. "Nonlinear dynamics and chaos. 1994." Reading: Perseus Books.

Tesi, A., E. Abed, et al. (1996). "Harmonic balance analysis of period-doubling bifurcations with implications for control of nonlinear dynamics." Automatica **32**(9): 1255-1271.

Tsihrintzis, G. A. and C. L. Nikias (1995). "Performance of optimum and suboptimum receivers in the presence of impulsive noise modeled as an alpha-stable process." Communications, IEEE Transactions on **43**(234): 904-914.

Tsihrintzis, G. A. and C. L. Nikias (1996). "Fast estimation of the parameters of alpha-stable impulsive interference." Signal Processing, IEEE Transactions on **44**(6): 1492-1503.

Vilar, J. M. G. and J. Rubi (1997). "Stochastic multiresonance." Physical Review Letters **78**(15): 2882-2885.